Original Article

Association of Genetic Polymorphisms of Endothelin-Converting Enzyme-1 Gene with Hypertension in a Japanese Population and Rare Missense Mutation in Preproendothelin-1 in Japanese Hypertensives

Mariko BANNO[1),2)], Hironori HANADA[1)], Kei KAMIDE[3)], Yoshihiro KOKUBO[4)], Akiko KADA[1)], Jin YANG[1),3)], Chihiro TANAKA[1)], Shin TAKIUCHI[3)], Takeshi HORIO[3)], Tetsutaro MATAYOSHI[3)], Hisayo YASUDA[3)], Junko NAGURA[4)], Hitonobu TOMOIKE[4)], Yuhei KAWANO[3)], and Toshiyuki MIYATA[1)]

Endothelin-1 (EDN1), a 21-amino acid peptide, is a potent vasoconstrictor with various pharmacological responses. EDN1 is synthesized from a 212-amino acid precursor protein, preproEDN1, through multiple proteolytic steps. Endothelin-converting enzyme (ECE) cleaves a Trp73–Val74 peptide bond in big-EDN1 to give rise to mature EDN1. In this study, we examined the possible association of genetic variations in *ECE1* with hypertension in a general Japanese population and searched for missense mutations in and around the EDN1 polypeptide. We genotyped 5 single nucleotide polymorphisms (SNPs) in the *ECE1* gene in 1,873 individuals from a general Japanese population and identified one SNP associated with hypertension in women (rs212528: TT *vs.* TC+CC: odds ratio=1.40; 95% confidence intervals: 1.04–1.89; p=0.026), after adjusting for confounding factors. The systolic blood pressure in women with the CC genotype was 6.44 mmHg higher than that in those with the TT genotype (p=0.007), after adjusting for the same factors. Next, to identify the missense mutations that may influence the biological activity of EDN1, we sequenced the genomic region that encodes EDN1 in 942 Japanese hypertensive patients. We identified a novel missense mutation, G36R, in one hypertensive patient, but no mutations were observed in EDN1. A gene polymorphism in *EDN1*, Lys198Asn, has been reported to be associated with hypertension in obese subjects. Taken together, these findings reveal that the EDN-ECE pathway is an important system involved in essential hypertension in Japanese. (*Hypertens Res* 2007; 30: 513–520)

***Key Words*: endothelin, endothelin-converting enzyme, gene variants, hypertension, general population**

From the [1)]Research Institute, Divisions of [3)]Hypertension and Nephrology and [4)]Preventive Cardiology, National Cardiovascular Center, Suita, Japan; and [2)]Department of Information, Environmental and Food Sciences, Faculty of Education, Art and Sciences, Yamagata University, Yamagata, Japan.

This study was supported by the Program for Promotion of Fundamental Studies in Health Science of the Pharmaceuticals and Medical Devices Agency (PMDA), the Program for Promotion of Fundamental Studies in Health Sciences of the National Institute of Biomedical Innovation (NIBIO) of Japan and a Grant-in-Aid from the Ministry of Health, Labor, and Welfare of Japan and a Grant-in-Aid for Scientific Research from the Ministry of Education, Culture, Sports, Science, and Technology of Japan.

Address for Reprints: Kei Kamide, M.D., Ph.D., Division of Hypertension and Nephrology, National Cardiovascular Center, 5–7–1 Fujishirodai, Suita 565–8565, Japan. E-mail: kamide@hsp.ncvc.go.jp

Received December 28, 2005; Accepted in revised form January 25, 2007.

Introduction

The endothelin (EDN) system is comprised of 4 active EDNs, with EDN1 being the predominant isoform in the cardiovascular system (*1*). Because of the potent vasoconstricting and mitogenic effects of EDN1 and its involvement in various cardiovascular diseases, biosynthesis of EDN1 has received considerable attention. EDN1 is synthesized from a 212-amino acid precursor protein, preproEDN1, through multiple proteolytic steps. In the first step, preproEDN1 is cleaved by a signal peptidase, resulting in the formation of proEDN1, which is then cleaved by a furin-like enzyme to yield the 38-amino acid protein known as big-EDN1 (amino acids 53–92) or other intermediates. Big-EDN1 is subsequently cleaved by a unique type II metalloprotease, EDN-converting enzyme-1 (ECE1), to yield EDN1 (amino acids 53–73) (*2*).

The EDN system is a promising target for the genetic analysis for hypertension. The missense mutation Lys198Asn has been identified in preproEDN1, and several reports have described that this polymorphism showed a positive association with blood pressure elevation in overweight people (*3–5*), although no significant difference in the EDN1 levels between the Asn-type and Lys-type transfectant was observed in an expression analysis (*6*). As for *ECE1*, an association between the −338C>A polymorphism in *ECE1* and blood pressure levels in women but not in men has recently been reported (*7*). This C>A polymorphism is associated with increased promoter activity, as demonstrated in a promoter assay analysis (*8*).

Complex traits such as hypertension, diabetes mellitus, and hyperlipidemia are suggested to be caused by common sequence variants that may have a small to moderate phenotypic effect (*9–11*). On the other hand, accumulating data has shown that most Mendelian disorders are caused by a set of different mutations that often reside in coding regions. These rare variants tend to have strong phenotypic effects. Several recent studies have shown that rare genetic variations in *ABCA1*, *APOA1*, and *LCAT* collectively contribute to the variation in plasma levels of high-density lipoprotein (HDL) cholesterol in the general population (*12*, *13*). We hypothesized that rare genetic variations in hypertension candidate genes could collectively contribute to hypertension. To investigate this hypothesis, we have been identifying such mutations in Japanese hypertensive subjects; to date, we have identified missense mutations in the β- or γ-subunit of the amiloride-sensitive epithelial sodium channel encoded by *SCNN1B* and *SCNN1G* (*14*), a causative gene for pseudohypoaldosteronism type II encoded by serine-threonine kinase *WNK4* (*15*), the regulator of G-protein signaling 2 (*RGS2*) (*16*), and the mineralocorticoid receptor encoded by *NR3C2* (*17*). As the next hypertension candidate gene, we have begun to sequence the *EDN1* gene and to search for missense mutations (*18*).

In present study, we genotyped the genetic polymorphisms of one of the EDN-converting enzymes, the *ECE1* gene, in a general Japanese population to examine whether the *ECE1* gene is a susceptibility gene for hypertension. Secondly, to evaluate the EDN system in essential hypertension in Japanese, we re-sequenced the EDN1 polypeptide in the *EDN1* gene in Japanese hypertensive patients to identify missense mutations that may deleteriously affect EDN1 function.

Methods

General Population

The selection criteria and design of the Suita study have been described previously (*19*, *20*). Only those who gave written informed consent for genetic analyses were included in this study. The study protocol was approved by the Ethical Review Committee of the National Cardiovascular Center. In this study, the genotypes of 1,873 samples were determined. The characteristics of the 1,873 participants (863 men and 1,010 women) are shown in Table 1. Routine blood examinations that included total serum cholesterol, HDL cholesterol, triglyceride, and glucose levels were performed. A physician or nurse interviewed each patient regarding smoking and alcohol drinking habits and personal history of cardiovascular disease, including angina pectoris, myocardial infarction, and/or stroke. Blood pressure was measured after at least 10 min of rest in a sitting position. Systolic and diastolic blood pressures (SBP and DBP) were the means of two measurements by well-trained doctors (recorded >3 min apart). Hypertension was defined as SBP of ≥140 mmHg, DBP of ≥90 mmHg, or the current use of antihypertensive medication (*20*). Diabetes mellitus was defined as fasting plasma glucose ≥7.0 mmol/L (126 mg/dL), non-fasting plasma glucose ≥11.1 mmol/L (200 mg/dL), current use of antidiabetic medication, or HbA1c ≥6.5%. Hyperlipidemia was defined as total cholesterol ≥5.68 mmol/L (220 mg/dL) or antihyperlipidemia medication. Body mass index (BMI) was calculated as weight (in kg) divided by height (in m) squared.

Hypertensive Subjects

A total of 942 hypertensive subjects (518 men and 424 women; average age: 65.1±10.5 years) were recruited from the Division of Hypertension and Nephrology at the National Cardiovascular Center. Ninety-two percent of study subjects (870 subjects) were diagnosed with essential hypertension, and the rest had secondary hypertension, including renal hypertension (36 subjects), renovascular hypertension (23 subjects), primary aldosteronism (11 subjects) and hypothyroid-induced hypertension (2 subjects) (*14–17*). The hypertension criteria were blood pressure above 140 and/or 90 mmHg or the use of antihypertensive agents. Blood pressure was the average of three measurements taken in a sitting position after at least 5 min of rest on each occasion. About one-third of the hypertensive subjects had hypertensive cardiovas-

Table 1. Basic Characteristics of Subjects in Japanese General Population (Suita Study)

	Women (n=1,010)	Men (n=863)
Age (yeasr old)	63.3±11.0	66.3±11.1*
Systolic blood pressure (mmHg)	128.0±19.6	131.9±19.5*
Diastolic blood pressure (mmHg)	76.6±9.8	79.7±10.7*
Body mass index (kg/m^2)	22.3±3.2	23.3±3.0*
Total cholesterol (mmol/L)	5.57±0.79*	5.10±0.78
HDL-cholesterol (mmol/L)	1.67±0.40*	1.42±0.36
Current smokers (%)	6.3	30.1†
Current drinkers (%)	29.3	67.0†
Present illness (%)		
Hypertension	38.2	47.4†
Hyperlipidemia	55.2†	27.4
Diabetes mellitus	5.2	12.6†

Values are mean±SD or percentage. Hypertension: systolic blood pressure ≥140 mmHg and/or diastolic blood pressure ≥90 mmHg or antihypertensive medication; hyperlipidemia: total cholesterol ≥220 mg/dL or antihyperlipidemia medication; diabetes: fasting plasma glucose ≥126 mg/dL or non-fasting plasma glucose ≥200 mg/dL or HbA1c ≥6.5% or antidiabetic medication. *$p<0.05$ between women and men by Student's t-test. †$p<0.05$ between women and men by χ^2 test. HDL, high-density lipoprotein.

Table 2. General Characteristics of Patients with Hypertension and/or Renal Failure

Number	942
Age (years)	65.1±10.5
Gender (M/F)	518/424
Body mass index (kg/m^2)	24.2±3.3
Systolic blood pressure (mmHg)	145.5±19.2
Diastolic blood pressure (mmHg)	84.8±13.4
Essential hypertension	870
Secondary hypertension	72
Renal hypertension	36
Renovascular hypertension	23
Primary aldosteronism	11
Hypothyroid-induced hypertension	2
Renal impairment*	110
Ischemic heart disease	102
Stroke**	145

Values are expressed as mean±SD. *Patients who had serum creatinine ≥1.4 mg/dL. **Silent cerebral infarction was included. M, male; F, female.

cular complications. The clinical features of the patients in this study are summarized in Table 2.

All of the participants for the genetic analysis in the present study gave their written informed consent. The study protocol was approved by the Ethical Review Committee of the National Cardiovascular Center.

Genotyping of Mutations of Single Nucleotide Polymorphisms of the *ECE1* Gene in the General Population

We obtained genetic polymorphisms in the *ECE1* gene using the database of Japanese Single Nucleotide Polymorphisms (JSNP) (http://snp.ims.u-tokyo.ac.jp/) (*21*, *22*) and genotyped the following 5 single nucleotide polymorphisms (SNPs) by the TaqMan-PCR system: rs212548-TC (IMS-JST017298 in intron 4), rs212528-TC (IMS-JST004319 in intron 5), rs212526-CT (IMS-JST009090 in intron 6), rs2038090-AC (IMS-JST004325 in intron 17), and rs2038089-AG (IMS-JST004324 in intron 17). The primers and probes of the TaqMan-PCR system are available on request. Hereafter, SNPs are described according to the RS nomenclature system.

Screening of Mutations in Exon 2 of the *EDN1* Gene

Blood samples were obtained from each subject and genomic DNA was isolated from peripheral blood leukocytes using an NA-3000 nucleic acid isolation system (KURABO, Osaka, Japan). The region of exon 2 was amplified by polymerase chain reaction (PCR) using a pair of specific primers, 5′-CTGATGGCAGGCTGTGTGCTT-3′ and 5′-CCCCATCAG ATGCCACTGTGA-3′, which flank the 612-bp region containing exon 2. The PCR products were directly sequenced on an ABI PRISM 3700 DNA analyzer (Applied Biosystems, Foster City, USA) as described previously (*23*, *24*). The obtained sequences were examined for the presence of mutations using Sequencher software (Gene Codes Corporation, Ann Arbor, USA), followed by visual inspection (*25*).

Statistical Analysis

Analysis of variance was used to compare mean values between groups, and if overall significance was demonstrated, the intergroup difference was assessed by means of a general linear model. Frequencies were compared by χ^2 analysis. Association analyses between genotypes and blood pressure in each sex were performed through logistic regression analysis with consideration for potential confounding risk variables, including age, BMI, present illness (hyperlipidemia and diabetes mellitus), lifestyle (smoking and drinking), and antihypertensive medication. For multivariate risk predictors, the adjusted odds ratios were given with the 95% confidence intervals. The relationship between genotypes and risk of hypertension was expressed in terms of the odds ratios adjusted for possible confounding effects, including age, BMI, present illness (hyperlipidemia and diabetes mellitus), and lifestyle (smoking and drinking). Odds ratios were calculated as a measure of the association between each genotype

Table 3. Odds Ratio of Polymorphisms in *ECE1*

SNP	Sex	Genotype	*n*	Odds ratio	(95% CI)	*p*	Genotype	*n*	Odds ratio	(95% CI)	*p*
rs212548	Women	TT	328	1	(reference)		TT+TC	821	1	(reference)	
		TC+CC	686	1.28	(0.94–1.74)	0.116	CC	193	1.21	(0.85–1.72)	0.293
	Men	TT	275	1	(reference)		TT+TC	692	1	(reference)	
		TC+CC	590	1.10	(0.82–1.50)	0.520	CC	173	0.98	(0.69–1.40)	0.924
rs212528	Women	TT	663	1	(reference)		TT+TC	980	1	(reference)	
		TC+CC	347	1.40	(1.04–1.89)	0.026	CC	30	1.63	(0.74–3.58)	0.227
	Men	TT	528	1	(reference)		TT+TC	827	1	(reference)	
		TC+CC	335	0.83	(0.62–1.11)	0.198	CC	36	0.75	(0.37–1.53)	0.428
rs212526	Women	CC	734	1	(reference)		CC+CT	996	1	(reference)	
		CT+TT	280	0.76	(0.55–1.05)	0.099	TT	18	0.77	(0.25–2.35)	0.650
	Men	CC	615	1	(reference)		CC+CT	842	1	(reference)	
		CT+TT	251	0.95	(0.70–1.30)	0.751	TT	24	1.40	(0.58–3.38)	0.455
rs2038090	Women	AA	774	1	(reference)		AA+AC	999	1	(reference)	
		AC+CC	239	1.17	(0.84–1.64)	0.348	CC	14	1.05	(0.30–3.61)	0.939
	Men	AA	676	1	(reference)		AA+AC	856	1	(reference)	
		AC+CC	189	1.00	(0.71–1.40)	0.989	CC	9	3.32	(0.67–16.45)	0.142
rs2038089	Women	AA	414	1	(reference)		AA+AG	880	1	(reference)	
		AG+GG	598	1.19	(0.89–1.59)	0.240	GG	132	1.21	(0.80–1.84)	0.358
	Men	AA	380	1	(reference)		AA+AG	788	1	(reference)	
		AG+GG	486	1.12	(0.84–1.49)	0.450	GG	78	1.33	(0.81–2.18)	0.264

*Conditional logistic analysis, adjusted for age, body mass index, present illness (hyperlipidemia and diabetes mellitus), and lifestyle (smoking and drinking). SNP, single nucleotide polymorphism; CI, confidence interval.

Table 4. Association of Genotypes with Blood Pressure Variation

SNP	Genotype	Women					Men				
		n	DBP (mmHg)	*p**	SBP (mmHg)	*p**	*n*	DBP (mmHg)	*p**	SBP (mmHg)	*p**
rs212528	TT	663	76.49±0.37		126.89±0.64		528	79.98±0.43		131.94±0.75	
	TC	317	76.55±0.53		129.21±0.93		299	79.48±0.57		131.18±1.00	
	CC	30	77.57±1.72	0.698	133.33±3.02	0.007	36	80.93±1.66	0.931	133.83±2.89	0.941
	TT	663	76.49±0.37		126.89±0.64		528	79.98±0.43		131.94±0.75	
	TC+CC	347	76.63±0.51	0.823	129.56±0.89	0.016	335	79.64±0.54	0.840	131.47±0.94	0.698
	TT+TC	980	76.51±0.30		127.64±0.53		827	79.67±0.34		131.66±0.60	
	CC	30	77.57±1.72	0.545	133.33±3.02	0.066	36	80.93±1.66	0.458	133.83±2.89	0.463
rs212526	CC	734	76.56±0.35		128.07±0.61		615	79.41±0.40		131.67±0.69	
	CT	262	76.90±0.58		127.51±1.03		227	80.15±0.66		131.39±1.15	
	TT	18	70.08±2.19	0.344	120.04±3.87	0.175	24	84.13±2.06	0.048	138.16±3.59	0.422
	CC	734	76.56±0.35		128.07±0.61		615	79.41±0.40		131.67±0.69	
	CT+TT	280	76.45±0.56	0.874	127.02±0.99	0.371	251	80.52±0.63	0.135	132.03±1.09	0.780
	CC+CT	996	76.65±0.30		127.92±0.52		842	79.61±0.34		131.59±0.59	
	TT	18	70.08±2.19	0.003	120.04±3.87	0.044	24	84.13±2.06	0.030	138.16±3.59	0.071

Values are mean±SEM. *Conditional logistic analysis, adjusted for age, body mass index (BMI), present illness (hyperlipidemia and diabetes mellitus), and lifestyle (smoking and drinking). SNP, single nucleotide polymorphism; DBP, diastolic blood pressure; SBP, systolic blood pressure.

and hypertension under the assumption of a dominant (with scores of 0 for patients homozygous for the major allele and 1 for carriers of the minor allele) or recessive (with scores of 0 for carriers of the major allele and 1 for patients homozygous

Table 5. Haplotype Frequency (Freq) of *ECE1* Gene in Hypertensives (HT) and Normotensives (NT)

Haplotype		All				Men				Women			
		Freq (%)	χ^2	*p* Asymptotic	*p* Permutation	Freq (%)	χ^2	*p* Asymptotic	*p* Permutation	Freq (%)	χ^2	*p* Asymptotic	*p* Permutation
H1 T/T/C/A/A	Overall	19.2	1.278	0.258	0.327	19.0	0.040	0.841	0.893	19.3	2.954	0.086	0.127
	NT	19.8				18.8				20.4			
	HT	18.4				19.2				17.3			
H2 C/C/C/A/A	Overall	16.2	1.305	0.253	0.284	17.5	0.193	0.661	0.669	15.1	2.991	0.084	0.091
	NT	15.5				17.9				14.0			
	HT	16.9				17.1				16.9			
H3 T/T/C/A/G	Overall	14.3	0.122	0.727	0.769	14.7	0.231	0.631	0.695	14.2	0.060	0.807	0.825
	NT	14.1				14.4				14.0			
	HT	14.5				15.2				14.4			
H4 C/T/C/A/A	Overall	11.8	0.181	0.670	0.716	11.9	0.033	0.857	0.867	11.8	0.250	0.617	0.699
	NT	12.0				12.1				12.1			
	HT	11.5				11.8				11.4			
H5 T/T/T/A/A	Overall	10.7	8.254	0.004	0.015	10.9	0.421	0.516	0.575	10.6	11.865	0.001	0.003
	NT	12.0				11.4				12.4			
	HT	9.0				10.4				7.5			
H6 T/T/C/C/G	Overall	8.3	0.317	0.574	0.618	7.8	0.327	0.568	0.624	9.0	0.001	0.974	0.978
	NT	8.1				8.1				9.0			
	HT	8.7				7.3				9.0			
H7 C/T/C/A/G	Overall	7.8	0.133	0.715	0.775	6.2	1.115	0.291	0.402	8.8	2.071	0.150	0.192
	NT	7.6				5.5				8.2			
	HT	7.9				6.7				10.0			

Haplotypes (rs212548/rs212528/rs212526/rs2038090/rs2038089) with frequencies of more than 5% are shown. One hundred thousand replicates were used for permutation test for all, men and women. Numbers of haplotypes in Overall, NT, and HT are 3,736, 2,150, 1,586 for All; 1,730, 914, 816 for men; and 2,030, 1,254, 776 for women, respectively.

for the minor allele) mode of inheritance. The *p* values were adjusted by Bonferroni correction. SAS statistical software (release 6.12; SAS Institute Inc., Cary, USA) was used for the statistical analyses. The data of linkage disequilibrium, haplotype blocks and coverage of HapMap SNPs were downloaded from the HapMap Consortium (http://www.hapmap.org). Haplotypes and permutation analyses were calculated using SNPAlyze version 4.0 software (DYNACOM Co., Mobara, Japan).

Results

Association between SNPs in the *ECE1* Gene and Hypertension

Five genetic polymorphisms in the *ECE1* gene were genotyped in 1,873 individuals. The genotype frequencies for each polymorphism were as follows: rs212548-T>C, 0.563/0.437; rs212528-T>C, 0.800/0.200; rs212526-C>T, 0848/0.152; rs2038090-A>C, 0.880/0.120; rs2038089-A>G, 0.655/0.345. None of the genotype frequencies were significantly different from those expected from the Hardy-Weinberg equilibrium ($p>0.05$). Multiple logistic regression analysis after adjusting for confounding factors of age, BMI, hyperlipidemia, diabetes mellitus, smoking, and drinking revealed that one polymorphism, rs212528, in intron 5 was significantly associated with hypertension in women (rs212528-T>C: TT *vs.* TC+CC; odds ratio=1.40; 95% confidence interval: 1.04–1.89; $p=0.026$) (Table 3). The SBPs in women with the TT, TC, and CC genotypes were 126.89±0.64 mmHg ($n=663$), 129.21±0.93 mmHg ($n=317$), and 133.33±3.02 mmHg ($n=30$) ($p=0.007$), after adjusting for the same confounding factors (Table 4). Thus, the difference in SBP was 6.44 mmHg between women with the CC genotype and those with the TT genotype. This association was still significant even after the Bonferroni correction.

Another polymorphism, rs212526, was associated with a significant difference in DBP: women having the CC+CT genotype had a DBP of 76.65±0.30 mmHg ($n=996$) and those with the TT genotype had a DBP of 70.08±2.19 mmHg ($n=18$) ($p=0.003$) after adjusting for the same confounding factors (Table 4). This polymorphism was also significantly associated with the SBP in women (CC+CT: 127.92±0.52 mmHg, $n=996$; TT: 120.04±3.87 mmHg, $n=18$; $p=0.044$). However, this polymorphism did not show a significant association with hypertension. In men, this polymorphism was

Table 6. List of 5 Polymorphisms and Their Allele Frequency in Exon 2 of *EDN1* Identified by Direct Sequencing of 942 Hypertensive Japanese

Allele 1 > allele 2	Amino acid change	region	Allele frequency		Flanking sequence	rs ID
			Allele 1	Allele 2		
1753G>A	G36R	exon 2	1.000	0.000	TGAGAACGGC[G/A]GGGAGAAACC	
1910G>T		intron 2	0.473	0.527	TGTAACCCTA[G/T]TCATTCATTA	rs2070699
1918T>A		intron 2	0.999	0.001	TAGTCATTCA[T/A]TAGCGCTGGC	
2008G>A		intron 2	0.999	0.001	GTGCCTCAGT[G/A]GGGACAGTTT	
2107G>A		intron 2	0.999	0.001	TACTCATGAT[G/A]GGACAAGCAG	

The A of the ATG of the initiator Met codon is denoted nucleotide +1, as recommended by the Nomenclature Working Group (*28*). The nucleotide number was according to the reference sequences GenBank Accession ID: NT_007592.

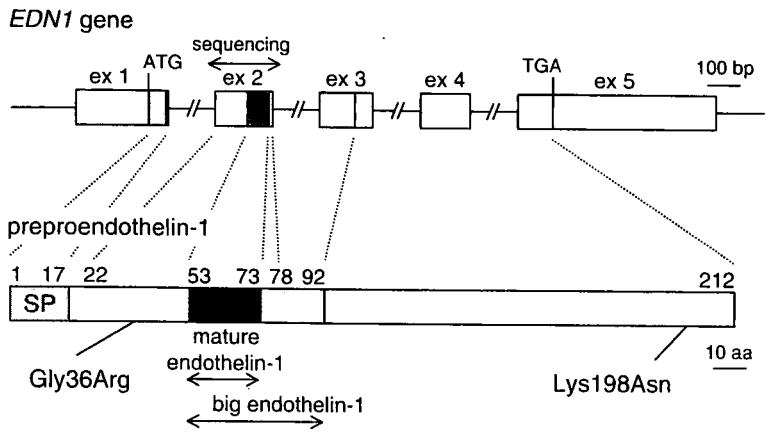

Fig. 1. *Genome and domain structure of human endothelin 1. Two missense mutations in endothelin-1, Gly36Arg (G36R) and Lys198Asn (K198N), are shown. The G36R mutation in preproendothelin-1 was identified in this study.*

significantly associated with DBP (CC+CT: 79.61±0.34 mmHg, n=842; TT: 84.13±2.06 mmHg, n=24; p=0.030).

The haplotypes composed of the 5 SNPs genotyped in this study are shown in Table 5. Seven inferred haplotypes with frequencies of more than 5% were examined to determine their association with hypertension in all patients and in two sub-populations (men and women). In women, the frequency of haplotype H5 in the hypertensive group was significantly lower than that in the normotensive group.

A Novel Missense Mutation in the preproEDN1 Polypeptide in Japanese Hypertensives

We sequenced the region of exon 2 of *EDN1* in 942 hypertensive patients with strong genetic background and secondary hypertension. The results are shown in Table 6. In this study, we were not able to detect any missense mutations within the mature EDN1 region. However, we identified one novel missense mutation, G36R, in *EDN1* in a heterozygous form in a male patient. The prevalence of this mutation was 0.05% in our Japanese hypertensive population. We tried to screen this missense mutation, G36R in *EDN1*, in our general population by the TaqMan-PCR method, but this genotyping failed due to technical problems.

Discussion

In this study, we used two different approaches to reveal the contribution of the EDN system to hypertension in two different populations, a general population and a hypertensive population, both from the Osaka region in Japan.

We genotyped 5 SNPs in *ECE1* and identified rs212528 as the hypertension/blood pressure susceptibility genetic variant. We used the currently available HapMap data from CHB-JPN to assess the coverage of haplotype blocks across the *ECE1* gene by 5 SNPs. The *ECE1* gene consisted of 6 haplotype blocks, in which rs212548 was present in block 2, two SNPs, rs212528 and rs212526, were present in block 3, and two SNPs, rs2038090 and rs2038089, were present in block 6, and the genotyped SNPs were estimated to cover approximately 90% of the haplotypes in block 2, 30% of those in block 3, and 90% of those in block 6, respectively. Two SNPs, rs212528 and rs212526, in block 3 had an r^2 of 0.031 and LOD score of 0.43, and rs2038090 and rs2038089 in block 6 had an r^2 of 0.163 and LOD score of 2.33.

In this study, the rs212528-T>C polymorphism in *ECE1* in

women was identified as the SNP conferring susceptibility for hypertension and blood pressure change. It is well known that the incidence of coronary artery disease shows a gender difference that may in part be related to the female sex hormones estrogen and progesterone. The literature provides evidence that estrogen inhibits EDN1 production (*26*). Furthermore, estrogen inhibits ECE-1 mRNA expression (*27*). These findings may explain the gender difference of *ECE1* polymorphisms for hypertension. The mean age of women in our population was 63.3 years. Despite the relatively advanced age of this population, we identified a contribution of the rs212528 polymorphism to hypertension and blood pressure change, while haplotypes containing the rs212528-C allele were not clearly associated with normotension or hypertension. The association might have been stronger if we had used a younger female population.

Another polymorphism, rs212526-C>T in intron 6, was associated with a blood pressure change in women and men. The mean DBP of the 996 women with the CC+CT genotype was 6.57 mmHg higher than that of the 18 women with the TT genotype ($p=0.003$), and the SBP change also showed the same trend—that is, women with the CC+CT genotype had higher blood pressure than women with the TT genotype ($p=0.044$) (Table 4). However, in men, the opposite trend was seen. The mean DBP of the 842 men with the CC+CT genotype was 4.52 mmHg lower than that of the 24 men with the TT genotype ($p=0.030$). Haplotype H5 containing the rs212528-T allele was significantly more prevalent in the normotensive group. This association also suggested that the T-allele of rs212528 was involved in blood pressure in women (Tables 3–5). Thus, the significance of rs212526 on blood pressure change should be evaluated using other population.

The association of SNP with hypertension and blood pressure change is at best marginally significant given the number of tests performed. All the *p*-values were more than 0.007. However, rs212528 is present in the *ECE1* gene, which encodes the endothelin-converting enzyme. In addition, this SNP showed a positive association with both hypertension and blood pressure change. Thus, we regarded this SNP as a hypertension candidate. SNP and blood pressure/hypertension described in the present study needs to be confirmed by another set of studies.

In the hypertensive population, we sequenced the coding region of the EDN1 polypeptide and its flanking region in 942 Japanese hypertensives and identified one novel missense mutation, G36R, that was not present in the EDN1 polypeptide but was present in the preproEDN-1 region (Fig. 1). At present, the effect of G36R mutation on the EDN1 function is not clear, because it was located far from the scissile site, the R52–C53 bond, by the furin-like enzyme. From the evolutionary point of view, G36 was conserved in humans, chimpanzees, cows, and dogs, but mice and rats have Val and chickens have Ala. The arginine residue at position 36 was not found in preproEDN1 in any species. To reveal the functional effect of this missense mutation on the processing of preproEDN1, an expression study of the mutant preproEDN1 is needed.

We have hypothesized that rare nonsynomymous mutations in candidate genes could collectively contribute to complex traits. In this model, the extensive sequence-based approaches focusing on identification of these mutations is necessary. So far, we have sequenced several hypertension candidate genes to evaluate whether rare variants could contribute to the etiology of hypertension. At present, however, whether rare variants contribute to hypertension is not clear due to the lack of *in vitro* or *in vivo* expression studies of the mutant protein (*14*, *15*, *17*). The exception was the nonsense mutation identified in the *RGS2* gene, which has been clearly shown to produce the defective protein (*16*). In this study, we identified one missense mutation, G36R, in preproEDN1. The further collection of such missense mutations in hypertension candidate genes could lead to an enhanced understanding of the etiology of essential hypertension.

In summary, we revealed that the rs212528 polymorphism in *ECE1* was associated with hypertension and blood pressure change. In earlier reports, the Lys198Asn polymorphism in *EDN1* showed a positive association with blood pressure elevation in overweight people (*3–5*). Thus, endothelin family gene polymorphisms might play an important role in the etiology of essential hypertension.

Acknowledgements

We would like to express our gratitude to Dr. Otosaburo Hishikawa, Dr. Katsuyuki Kawasaki, Mr. Tadashi Fujikawa, and the members of the Satsuki-Junyukai for their continuous support of our population survey in Suita City. We also thank all the staff in the Division of Preventive Cardiology for their help with the medical examination.

References

1. Yanagisawa M, Kurihara H, Kimura S, *et al*: A novel potent vasoconstrictor peptide produced by vascular endothelial cells. *Nature* 1988; **332**: 411–415.
2. Miyauchi T, Masaki T: Pathophysiology of endothelin in the cardiovascular system. *Annu Rev Physiol* 1999; **61**: 391–415.
3. Tiret L, Poirier O, Hallet V, *et al*: The Lys198Asn polymorphism in the endothelin-1 gene is associated with blood pressure in overweight people. *Hypertension* 1999; **33**: 1169–1174.
4. Asai T, Ohkubo T, Katsuya T, *et al*: Endothelin-1 gene variant associates with blood pressure in obese Japanese subjects: the Ohasama Study. *Hypertension* 2001; **38**: 1321–1324.
5. Jin JJ, Nakura J, Wu Z, *et al*: Association of endothelin-1 gene variant with hypertension. *Hypertension* 2003; **41**: 163–167.
6. Tanaka C, Kamide K, Takiuchi S, *et al*: Evaluation of the Lys198Asn and −134delA genetic polymorphisms of the endothelin-1 gene. *Hypertens Res* 2004; **27**: 367–371.

7. Funalot B, Courbon D, Brousseau T, *et al*: Genes encoding endothelin-converting enzyme-1 and endothelin-1 interact to influence blood pressure in women: the EVA study. *J Hypertens* 2004; **22**: 739–743.
8. Funke-Kaiser H, Reichenberger F, Kopke K, *et al*: Differential binding of transcription factor E2F-2 to the endothelin-converting enzyme-1b promoter affects blood pressure regulation. *Hum Mol Genet* 2003; **12**: 423–433.
9. Risch N, Merikangas K: The future of genetic studies of complex human diseases. *Science* 1996; **273**: 1516–1517.
10. Collins FS, Guyer MS, Charkravarti A: Variations on a theme: cataloging human DNA sequence variation. *Science* 1997; **278**: 1580–1581.
11. Lander ES: The new genomics: global views of biology. *Science* 1996; **274**: 536–539.
12. Cohen JC, Kiss RS, Pertsemlidis A, *et al*: Multiple rare alleles contribute to low plasma levels of HDL cholesterol. *Science* 2004; **305**: 869–872.
13. Frikke-Schmidt R, Nordestgaard BG, Jensen GB, *et al*: Genetic variation in ABC transporter A1 contributes to HDL cholesterol in the general population. *J Clin Invest* 2004; **114**: 1343–1353.
14. Kamide K, Tanaka C, Takiuchi S, *et al*: Six missense mutations of the epithelial sodium channel β and γ subunits in Japanese hypertensives. *Hypertens Res* 2004; **27**: 333–338.
15. Kamide K, Takiuchi S, Tanaka C, *et al*: Three novel missense mutations of *WNK4*, a kinase mutated in inherited hypertension, in Japanese hypertensives: implication of clinical phenotypes. *Am J Hypertens* 2004; **17**: 446–449.
16. Yang J, Kamide K, Kokubo Y, *et al*: Genetic variations of regulator of G-protein signaling 2 in hypertensive patients and in the general population. *J Hypertens* 2005; **23**: 1497–1505.
17. Kamide K, Yang J, Kokubo Y, *et al*: A novel missense mutation, F826Y, in the mineralocorticoid receptor gene in Japanese hypertensives: implication of clinical phenotypes. *Hypertens Res* 2005; **28**: 703–709.
18. Vanhoutte PM, Feletou M, Taddei S: Endothelium-dependent contractions in hypertension. *Br J Pharmacol* 2005; **144**: 449–458.
19. Mannami T, Baba S, Ogata J: Strong and significant relationships between aggregation of major coronary risk factors and the acceleration of carotid atherosclerosis in the general population of a Japanese city: the Suita Study. *Arch Intern Med* 2000; **160**: 2297–2303.
20. Kokubo Y, Inamoto N, Tomoike H, *et al*: Association of genetic polymorphisms of sodium-calcium exchanger 1 gene, *NCX1*, with hypertension in a Japanese general population. *Hypertens Res* 2004; **27**: 697–702.
21. Haga H, Yamada R, Ohnishi Y, *et al*: Gene-based SNP discovery as part of the Japanese Millennium Genome Project: identification of 190,562 genetic variations in the human genome. Single-nucleotide polymorphism. *J Hum Genet* 2002; **47**: 605–610.
22. Hirakawa M, Tanaka T, Hashimoto Y, *et al*: JSNP: a database of common gene variations in the Japanese population. *Nucleic Acids Res* 2002; **30**: 158–162.
23. Okuda T, Fujioka Y, Kamide K, *et al*: Verification of 525 coding SNPs in 179 hypertension candidate genes in the Japanese population: identification of 159 SNPs in 93 genes. *J Hum Genet* 2002; **47**: 387–394.
24. Matayoshi T, Kamide K, Takiuchi S, *et al*: The thiazide-sensitive Na^+-Cl^- cotransporter gene, *C1784T*, and adrenergic receptor-β3 gene, *T727C*, may be gene polymorphisms susceptible to the antihypertensive effect of thiazide diuretics. *Hypertens Res* 2004; **27**: 821–833.
25. Kokubo Y, Kamide K, Inamoto N, *et al*: Identification of 108 SNPs in *TSC*, *WNK1*, and *WNK4* and their association with hypertension in a Japanese general population. *J Hum Genet* 2004; **49**: 507–515.
26. Webb CM, Ghatei MA, McNeill JG, *et al*: 17β-Estradiol decreases endothelin-1 levels in the coronary circulation of postmenopausal women with coronary artery disease. *Circulation* 2000; **102**: 1617–1622.
27. Rodrigo MC, Martin DS and Eyster KM: Vascular ECE-1 mRNA expression decreases in response to estrogens. *Life Sci* 2003; **73**: 2973–2983.
28. Antonarakis SE, Nomenclature Working Group: Recommendations for a nomenclature system for human gene mutations. *Hum Mut* 1998; **11**: 1–3.

Age- and gender-related differences of plasma prothrombin activity levels

Toshiyuki Sakata[1], Akira Okamoto[1], Takashi Morita[2], Yoshihiro Kokubo[3], Kiyoshi Sato[1], Akira Okayama[3], Hitonobu Tomoike[3], Toshiyuki Miyata[4]

[1]Laboratory of Clinical Chemistry, National Cardiovascular Center, Suita, Osaka, Japan; [2]Department of Biochemistry, Meiji Pharmaceutical University, Kiyose, Tokyo, Japan; [3]Department of Preventive Cardiology and [4]Research Institute, National Cardiovascular Center, Suita, Osaka, Japan

Dear Sir,

Advancing age is an important risk factor for venous or arterial thrombosis in both sexes (1–3). Moreover, gender is associated with differences in the prothrombotic state and in the progression of atherosclerosis that occurs with aging (4, 5). Prothrombin is one of the dominant factors influencing thrombin generation (6), and the prothrombin G20210A mutation accompanied by an increased level of prothrombin poses a risk factor for venous or arterial thrombosis (7, 8). However, gender differences in age-related changes in plasma prothrombin activity have not been investigated until now. In the present study, we measured prothrombin activity in 742 individuals derived from a general Japanese population which was supposed to be free of prothrombin G20210A mutation (9).

The study population was composed of samples randomly selected from the residents of Suita, a city located in the second largest urban area in Japan (the Suita Study) (4). All subjects had been visiting the National Cardiovascular Center every two years since 1989 for regular health checkups. Only subjects who provided written informed consent to have a blood examination were enrolled in this study. We excluded subjects treated with oral anticoagulant therapy. Finally, 742 subjects, aged 36 to 85 years (mean age: 64 years), were included in this study. Spearman correlation analysis was used to assess the association between aging and the level of prothrombin activity within a given gender. For comparison between the two gender groups, the Mann-Whitney U test was used. Differences with a value of $p<0.01$ for the Spearman correlation analysis and $p<0.05$ for the Mann-Whitney U test were considered to be significant. Statistical calculations were performed using SPSS version 12.0 (SPSS Inc, Chicago, IL, USA). Prothrombin activity was measured according to a published method (10) with a modification. Briefly, 200 µl of 20 mM Tris-HCl, 0.14 M NaCl, pH 7.5 buffer containing 1 mg/ml of bovine serum albumin (TBSA) was added to 50 µl of plasma anticoagulated with 0.13% sodium citrate. Then, diluted plasma was incubated for 150 seconds at 37°C, and we detected ΔA/min at 405 nm after adding 50 µl of the reagent containing 6 mM $CaCl_2$, 0.5 mM Boc-Val-Pro-Arg-pNA as a thrombin substrate, 500 pM carinactivase-1 as a thrombin activator, and TBSA. Calibration was performed with a standard-human-plasma (Dade Behring GmbH, Marburg, Germany). The coefficient of intra-assay variation for prothrombin activity assay was 2.0%.

The mean ± SD of prothrombin activity level in men and women was 110.2 ± 17.0 (range: 54.5–158.5%) and 120.4 ± 17.4 (range: 57.5–194.4%), respectively. Figure 1 shows the age-related distribution (36–85 years) of prothrombin activity in 348 men (Fig. 1A) and 394 women (Fig. 1B). As a whole, a linear decrease of prothrombin activity level with age was observed in

Correspondence to:
Toshiyuki Sakata, PhD
Laboratory of Clinical Chemistry, National Cardiovascular Center
Fujishirodai 5–7–1, Suita, Osaka 565–8565, Japan
Tel.: +81 6 6833 5012 ext. 2296, Fax: +81 6 6835 1176
E-mail: tsakata@hsp.ncvc.go.jp

Received January 10, 2007
Accepted after revision March 20, 2007

Prepublished online May 3, 2007
doi:10.1160/TH07-01-0019

Thromb Haemost 2007; 97: 1052–1053

men (r=-0.34, p<0.0001), but not in women (r=-0.04, p=0.47). When prothrombin activity level was analyzed in 10-year age groups, significant decreases were observed in the men aged 46–55 years and 56–65 years (p<0.0001), aged 56–65 years and 76–85 years (p<0.05), and in the women aged 66–75 years and 76–85 years (p<0.0001). Levels of prothrombin activity were decreased in both sexes in the oldest age group (aged 76–85 years). With regards to gender-related change, the prothrombin activity level in the age group of 56–65 years, 66–75 years, and 76–85 years was significantly lower in men than in women.

In the present study, we showed the age-related decrease in the plasma prothrombin activity of men and gender-related change in the plasma prothrombin activity. These results contribute to the understanding of age-related hypercoagulability and to the practical institution of anticoagulant therapy in older patients. It has been established that thrombin generation increases with age in both sexes, evidenced by plasma prothrombin fragment F1+2 levels produced by the cleavage of prothrombin by factor Xa (11, 12). Age-related hypercoagulability does not likely stem from the prothrombin activity, because the prothrombin activity of men showed the age-related decrease, but it may result from some other mechanisms including decreased levels of anticoagulant proteins such as protein C and S (11, 13). We presented here the gender-related change of significantly lower prothrombin activity levels in men in the age of 56–85 years than in women. Men tend to develop thrombotic events including recurrent venous thrombosis (14), but this tendency was not related to the plasma level of prothrombin activity. Our work sheds further light on the point that, when considering relative hypercoagulability, gender-adjustment is necessary for the comparison of prothrombin activity levels.

With regards to anticoagulant therapy, the plasma levels of vitamin K-dependent coagulation factors decrease with increasing intensity of anticoagulation therapy (15). At the same time, the risks of major haemorrhage increase according to the intensity of anticoagulation therapy, especially in patients older than 80 years (16). Given our current study results, the markedly decreased prothrombin level in the age group of 76–85 years, especially in men, provides a potential mechanistic explanation for the increased rate of major haemorrhage observed in elderly patients receiving anticoagulant therapy.

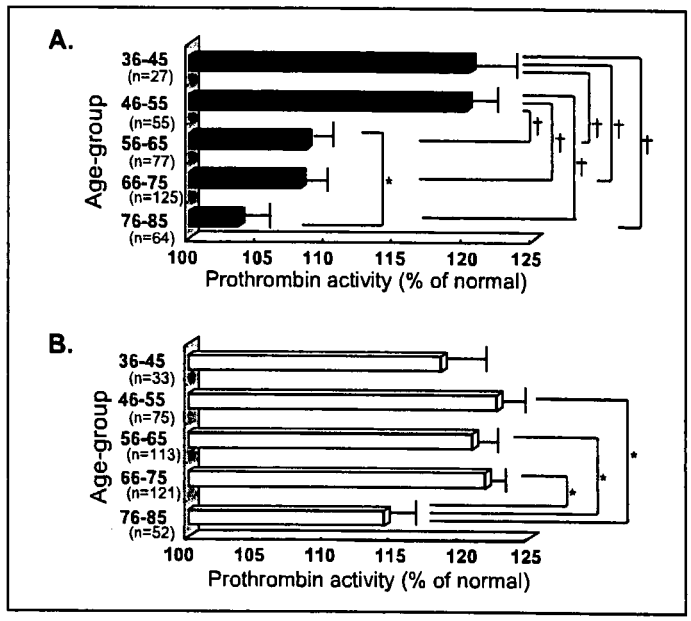

Figure 1: Age-related changes of plasma prothrombin activity levels according to gender (A: men, B: women). Populations aged from 36 to 85 years old were divided into five age groups by gender. Data are expressed as the mean ± SEM. *: P<0.05, †: P<0.0001, compared between two age groups of the same gender.

In conclusion, there are significant age- and gender-related differences in plasma prothrombin activity levels. In particular, the prothrombin activity level in men in the age group of 76–85 years was lower than that of any other age group in either gender.

Acknowledgments

This study was supported by the Program for Promotion of Fundamental Studies in Health Sciences of the National Institute of Biomedical Innovation (NIBIO), a Grant-in-Aid from the Ministry of Health, Labor, and Welfare of Japan, and the Ministry of Education, Culture, Sports, Science, and Technology of Japan.

References

1. White RH. The epidemiology of venous thromboembolism. Circulation 2003; 107: I4–8.
2. Feinbloom D, Bauer KA. Assessment of hemostatic risk factors in predicting arterial thrombotic events. Arterioscler Thromb Vasc Biol 2005; 25: 2043–2053.
3. Couturaud F, Kearon C, Leroyer C, et al. Incidence of venous thromboembolism in first-degree relatives of patients with venous thromboembolism who have factor V Leiden. Thromb Haemost 2006; 96: 744–749.
4. Mannami T, Baba S, Ogata J. Strong and significant relationships between aggregation of major coronary risk factors and the acceleration of carotid atherosclerosis in the general population of a Japanese city: the Suita Study. Arch Intern Med 2000; 160: 2297–2303.
5. Tofler GH, Massaro J, Levy D, et al. Relation of the prothrombotic state to increasing age (from the Framingham Offspring Study). Am J Cardiol 2005; 96: 1280–1283.
6. Butenas S, van't Veer C, Mann KG. "Normal" thrombin generation. Blood 1999; 94: 2169–2178.
7. Poort SR, Rosendaal FR, Reitsma PH, et al. A common genetic variation in the 3'-untranslated region of the prothrombin gene is associated with elevated plasma prothrombin levels and an increase in venous thrombosis. Blood 1996; 88: 3698–3703.
8. Ye Z, Liu EH, Higgins JP, et al. Seven haemostatic gene polymorphisms in coronary disease: meta-analysis of 66,155 cases and 91,307 controls. Lancet 2006; 367: 651–658.
9. Miyata T, Kawasaki T, Fujimura H, et al. The prothrombin gene G20210A mutation is not found among Japanese patients with deep vein thrombosis and healthy individuals. Blood Coagul Fibrinolysis 1998; 9: 451–452.
10. Yamada D, Morita T. CA-1 method, a novel assay for quantification of normal prothrombin using a Ca2+-dependent prothrombin activator, carinactivase-1. Thromb Res 1999; 94: 221–226.
11. Bauer KA, Weiss LM, Sparrow D, et al. Aging-associated changes in induces of thrombin generation and protein C activation in humans. J Clin Invest 1987; 80; 1527–1534.
12. Mari D, Mannucci PM, Coppola R, et al. Hypercoagulability in centenarians: the paradox of successful aging. Blood 1995; 85: 3144–3149.
13. Miyata T, Kimura R, Kokubo Y, et al. Genetic risk factors for deep vein thrombosis among Japanese: Importance of protein S K196E mutation. Int J Hematol 2006; 83; 217–223.
14. White RH, Dager WE, Zhou H, et al. Racial and gender differences in the incidence of recurrent venous thromboembolism. Thromb Haemost 2006; 96: 267–273.
15. Sakata T, Kario K, Matsuo T, et al. Suppression of plasma activated factor VII levels by warfarin therapy. Arterioscler Thromb Vasc Biol 1995; 15; 241–246.
16. White RH, McBurnie MA, Manolio T, et al. Oral anticoagulation in patients with atrial fibrillation: adherence with guidelines in an elderly cohort. Am J Med 1999; 106; 165–171.

Impaired Mast Cell Maturation and Degranulation and Attenuated Allergic Responses in Ndrg1-Deficient Mice[1]

Yoshitaka Taketomi,*† Kohei Sunaga,† Satoshi Tanaka,[2¶] Masanori Nakamura,‡ Satoru Arata,* Tomohiko Okuda,[3#] Tae-Chul Moon,˙ Hyeun-Wook Chang,˙ Yukihiko Sugimoto,[¶] Koichi Kokame,# Toshiyuki Miyata,# Makoto Murakami,†§** and Ichiro Kudo[4†]

We have previously reported that N-myc downstream regulated gene-1 (NDRG1) is an early inducible protein during the maturation of mouse bone marrow-derived mast cells (BMMCs) toward a connective tissue mast cell-like phenotype. To clarify the function of NDRG1 in mast cells and allergic responses, we herein analyzed mast cell-associated phenotypes of mice lacking the Ndrg1 gene. Allergic responses including IgE-mediated passive systemic and cutaneous anaphylactic reactions were markedly attenuated in Ndrg1-deficient mice as compared with those in wild-type mice. In Ndrg1-deficient mice, dermal and peritoneal mast cells were decreased in number and morphologically abnormal with impaired degranulating ability. Ex vivo, Ndrg1-deficient BMMCs cocultured with Swiss 3T3 fibroblasts in the presence of stem cell factor, a condition that facilitates the maturation of BMMCs toward a CTMC-like phenotype, displayed less exocytosis than replicate wild-type cells after the cross-linking of Fc•RI or stimulation with compound 48/80, even though the exocytotic response of IL-3-maintained, immature BMMCs from both genotypes was comparable. Unlike degranulation, the production of leukotriene and cytokines by cocultured BMMCs was unaffected by NDRG1 deficiency. Taken together, the altered phenotypes of Ndrg1-deficient mast cells both in vivo and ex vivo suggest that NDRG1 has roles in the terminal maturation and effector function (degranulation) of mast cells. The Journal of Immunology, 2007, 178: 7042–7053.

Mast cells have long been considered to serve primarily as important effector cells for acute IgE-associated allergic reactions such as anaphylaxis, rhinitis, and asthma. Mast cells are tissue-resident cells of hemopoietic origin, representing an important source of a variety of inflammatory mediators such as vasoactive amines, proteases, eicosanoids, cytokines, and chemokines. They orchestrate various aspects of the IgE-associated and even IgE-independent immune responses not only through the release of these mediators but also through cell-cell interaction by which they regulate the function of other cells.

It has been elucidated that mast cells originate from hemopoietic stem cells in vivo (1) or multipotential progenitors in vitro (2). Mast cell precursors circulate in the blood and migrate into connective or mucous tissues where they differentiate into mature mast cell phenotypes depending on the microenvironment of the tissue (3–6). Stem cell factor (SCF)[5] and its receptor c-kit are prerequisites for the homing and subsequent differentiation of mast cells in the whole tissue (7, 8), and the $\bullet_4\bullet_7$ integrin (9) and the chemokine receptor CXCR2 (10) have additional and profound influences on the basal homing, establishment, and maintenance of mast cells in the small intestine. However, the precise mechanism underlying the tissue-based maturation of mast cells is still a challenging area in this field of research.

Coculture of IL-3-maintained immature mouse bone marrow-derived mast cells (BMMCs), a progenitor population of mast cells, with fibroblasts is a useful system for analyzing certain aspects of change into a connective tissue mast cell (CTMC)-like phenotype (11–14). We have developed a unique mast cell maturation system by which BMMCs cocultured with Swiss 3T3 fibroblasts in the presence of soluble SCF alter their morphological and functional properties from an immature to a mature CTMC-like phenotype after only 4–6 days of coculture (14). Following cDNA subtraction between BMMCs before and after such coculture, we have identified N-myc downstream regulated gene-1 (NDRG1) as the most frequently induced gene during the maturation of BMMCs into a mature CTMC-like phenotype under these conditions (15, 16). Moreover, the overexpression of NDRG1 in the rat mastocytoma RBL-2H3 augments exocytotic degranulation in response to IgE-dependent and

*Center for Biotechnology, †Department of Health Chemistry, School of Pharmaceutical Sciences, and ‡Department of Oral Anatomy and Developmental Biology, School of Dentistry, Showa University, Tokyo, Japan; §Tokyo Metropolitan Institute of Medical Science, Tokyo, Japan; ¶Department of Physiological Chemistry, Faculty of Pharmaceutical Sciences, Kyoto University, Kyoto, Japan; ˙College of Pharmacy, Yeungnam University, Gyonsan, Korea; #National Cardiovascular Center Research Institute, Osaka, Japan; and **Precursory Research for Embryonic Science and Technology, Japan Science and Technology Agency, Saitama, Japan

Received for publication August 9, 2006. Accepted for publication February 27, 2007.

The costs of publication of this article were defrayed in part by the payment of page charges. This article must therefore be hereby marked advertisement in accordance with 18 U.S.C. Section 1734 solely to indicate this fact.

[1] This work was supported by a Showa University special grant-in-aid for innovative collaborative research projects and a special research grant-in-aid for development of characteristic education from the Ministry of Education, Culture, Sports, Science, and Technology of Japan. M.M. was supported by Precursory Research for Embryonic Science and Technology, Japan Science and Technology Agency.

[2] Current address: Department of Immunobiology, School of Pharmaceutical Sciences, Mukogawa Women's University, Hyogo, Japan.

[3] Current address: COE Formation for Genomic Analysis of Disease Model Animals with Multiple Genetic Alterations, Graduate School of Medicine, Kyoto University, Kyoto, Japan.

[4] Address correspondence and reprint requests to Dr. Ichiro Kudo, Department of Health Chemistry, School of Pharmaceutical Sciences, Showa University, 1-5-8 Hatanodai, Shinagawa-ku, Tokyo, Japan. E-mail address: ichi-ku@pharm.showa-u.ac.jp

[5] Abbreviations used in this paper: SCF, stem cell factor; NDRG1, N-myc downstream regulated gene-1; BMMC, bone marrow-derived mast cell; CMT4D, Charcot-Marie-Tooth disease type 4D; CPA, carboxypeptidase A; CTMC, connective tissue mast cell; HSA, human serum albumin; •-HEX, •-hexosaminidase; LT, leukotriene; lyso-PS, lysophosphatidyl-$_L$-serine; mMCP, mouse mast cell protease; PCA, passive cutaneous anaphylaxis; PLC, phospholipase C; PMC, peritoneal mast cell.

-independent stimuli (15), suggesting that NDRG1 is involved in the divergent signaling pathways leading to exocytosis at their point of convergence or beyond or that it allows immature mast cells to differentiate into a mature phenotype that degranulates more efficiently in response to various secretagogues.

NDRG1, an intracellular protein with an • • hydrolase fold (17) and three unique tandem repeats of 10 hydrophilic amino acids near the COOH-terminal end is a member of the emerging NDRG family that also contains NDRG2, NDRG3, and NDRG4 (18–20). NDRG1 has been independently identified as a molecule whose expression is markedly altered in several cell types under various conditions such as cellular stress response, hypoxia, and cell differentiation (15, 21–27). Significantly, the forcible expression of NDRG1 in cancer cells decreases their growth rate and metastasis by inducing cell differentiation and reversing their propensity to metastasize (28, 29), suggesting that NDRG1 is a cell differentiation regulator. Recently, a nonsense mutation in the Ndrg1 gene has been reported to be responsible for hereditary motor and sensory neuropathy-Lom, a severe autosomal recessive peripheral neuropathy known as Charcot-Marie-Tooth disease type 4D (CMT4D) (30, 31). Furthermore, mice lacking the Ndrg1 gene exhibit a peripheral neuropathy characterized by demyelination, a symptom similar to that observed in patients with CMT4D (32). These observations suggest that NDRG1 is essential for axon survival and appropriate differentiation, although the molecular machinery responsible for the neuronal function of NDRG1 still awaits further study.

To gain further insights into the functional role of this unique protein in mast cells, we have herein analyzed the mast cell-related phenotypes of Ndrg1-deficient mice. We found that the Ndrg1-deficient mice had mitigated passive systemic and local anaphylactic responses and that the mast cells from these mice were morphologically and functionally abnormal in terms of their aberrant granule structure and reduced exocytotic capacity. Thus, our findings provide unequivocal evidence that NDRG1 is a critical modulator of the maturation, and thereby the function, of mast cells.

Materials and Methods

Mice

The construction of the Ndrg1-deficient mice was described previously in detail (32). These Ndrg1-deficient mice were further backcrossed 10 generations onto a C57BL/6 background. All mice were bred in our animal facility under specific pathogen-free conditions. Mast cell-deficient WBB6F$_1$-W/W^v (W/W^v) and littermate control WBB6F$_1$-• /• mice were purchased from Japan SLC. We used 8- to 12-wk-old mice for all experiments. The genotypes of Ndrg1$^{•/}$ and Ndrg1$^{•/}$ were confirmed by PCR analysis of tail biopsies as described (32).

Passive systemic anaphylaxis

The anaphylaxis method used was described previously (33). Briefly, mice were administered 3 • g of anti-DNP mouse monoclonal IgE (SPE-7; Sigma-Aldrich) in 200 • l of saline i.v. through the tail vein. Then, 24 h later, the mice were challenged i.v. with 500 • g of DNP-conjugated human serum albumin (HSA) (DNP-HSA; Sigma-Aldrich) in 200 • l of saline. After Ag challenge, body temperature was monitored at various intervals using a rectal probe coupled to a digital thermometer (BAT-12R and RET-3; Physitemp Instruments). Blood samples were collected by puncturing the hearts of the sacrificed mice 1.5 min after Ag challenge. The sera were prepared and treated with 3% perchloric acid for the removal of proteins. The resulting supernatants were subjected to measurement of histamine. Histamine was separated by HPLC on a cation-exchange WCX-1 column (Shimadzu) and then measured fluorometrically by the o-phthalaldehyde method (34).

Passive cutaneous anaphylaxis (PCA)

The left and right ears of the mice were treated intradermally with 25 ng of anti-DNP IgE in 25 • l of saline. Then, 24 h later the mice were challenged i.v. through the tail vein with various doses of DNP-HSA together with 1 mg of Evans blue (Wako Pure Chemical) in 200 • l of saline. At various intervals after the Ag challenge, extravasation was visualized by blue staining of the ear skin. The ears were removed and incubated at 37°C in 1 ml of 3 N KOH. On the following day the mixtures were extracted with 1.24 M phosphoric acid and acetone. Absorbance of the resulting supernatants was measured at 620 nm. The relationship between Evans blue concentration and absorbance was linear, indicating that the absorbance represented the quantity of Evans blue extravasation. Ear thickness was recorded 30 min after Ag challenge using a dial thickness gauge (Mitutoyo Corporation) with a minimum sensitivity of 1 • m. Changes in ear thickness were determined as the difference before and after Ag challenge. For IgE-independent, compound 48/80-induced anaphylaxis, the ears were treated intradermally with various doses of compound 48/80 (Sigma-Aldrich) in 25 • l of saline followed by i.v. injection of 1 mg of Evans blue in 200 • l of saline. After 30 min, Evans blue extravasation was measured in a similar way.

Histological analysis

In a series of IgE-mediated, Ag-dependent PCA experiments, Ndrg1$^{•/}$ and Ndrg1$^{•/}$ mice were sacrificed before and after Ag challenge. The left and right ears were removed, fixed in 4% paraformaldehyde, and embedded in paraffin. Sections (5-• m thick) were cut and then stained with 0.05% acidic toluidine blue (pH 1.0). Intact and degranulated tissue mast cells were counted in the skin sections under an optical microscope (Axioskop 2 FS plus; Carl Zeiss MicroImaging) at • 100 magnification. Degranulated tissue mast cells were defined as those showing the release of • 10% cellular granules.

For transmission electron microscopy, ears were fixed with 2.5% glutaraldehyde in 0.1 M sodium cacodylate buffer (pH 7.2), postfixed with 2% OsO_4, dehydrated by a graded ethanol series, passed through propylene oxide, and then embedded in Epon 812. Ultrathin sections (0.08-• m thick) were stained with uranyl acetate and lead citrate and then examined using an electron microscope (H-7600; Hitachi).

For immunohistochemistry, cytospin preparations were incubated with 5% normal rabbit serum in PBS containing 5% BSA and 0.025% Triton X-100 for 1 h and then with goat anti-NDRG1 polyclonal Ab (N-19; Santa Cruz Biotechnology) at 1/100 dilution in the same buffer at 4°C overnight. These preparations were incubated with biotinylated rabbit anti-goat IgG (Vector Laboratories) at 1/100 dilution in PBS containing 5% BSA, 0.025% Triton X-100, and 10% mouse serum for 30 min followed by incubation with avidin DH and biotinylated HRP (Vectastain ABC kit; Vector Laboratories). After 30 min these preparations were stained with 0.5 mg/ml 3,3•-diaminobenzidine and 0.1% hydrogen peroxide solution.

Preparation and activation of peritoneal mast cells (PMCs)

To harvest peritoneal cells, 5 ml of HBSS was injected into the mouse peritoneal cavity and the abdomen was massaged gently. After the fluid containing peritoneal cells had been collected and centrifuged, the pellets were resuspended in PIPES-buffered saline. The cells were cytospun onto glass slides for 5 min and then incubated for 30 min with 1% Alcian blue (pH 2.5) and counterstained for 3 min with 0.1% safranin O.

For degranulation analysis, 10^6 peritoneal cells were incubated for 1 h in culture medium containing 100 ng/ml SCF and 10 • g/ml anti-DNP IgE and then treated for 30 min with 100 ng/ml DNP-BSA as an Ag and 4 • M 1-oleoyl-2-hydroxy-sn-glycero-3-phosphoryl-$_L$-serine (lyso-PS; Avanti Polar Lipids) as a cofactor in the same buffer. The contents of • -hexosaminidase (• -HEX) in both supernatants and cell pellets were then measured by triplicate. The percentage releases were calculated using the formula [S/(S • P)] • 100, where S and P are the • -HEX contents of the supernatants and cell pellets, respectively, from each sample. • -HEX assay was performed as described previously (35).

Analyses of protease activities

The chromogenic peptide substrates S-2586 (3-carbomethoxypropionyl-$_L$-arginyl-$_L$-propyl-$_L$-tyrosine-p-nitroaniline) and S-2288 (H-$_D$-isoleucyl-$_L$-propyl-arginine-p-nitroaniline) were purchased from Chromogenix, and M-2245 (N-(4-methoxyphenylazoformyl)-Phe-OH) from Bachem.

Ear extracts were obtained by the addition of 1 ml of PBS containing 2 M NaCl per ear, followed by homogenization using a PT3100 Polytron device (Kinematica). After homogenization, Triton X-100 was added to give a final concentration of 0.5%. The extracts were centrifuged at 10,000 • g, and 10-• l aliquots of the resultant supernatants were diluted with 90 • l of H_2O followed by incubation with 20 • l of 1.8 mM solution (in H_2O) of the chromogenic substrates S-2586 (for chymotrypsin-like proteases), S-2288 (for trypsin-like proteases), and M-2245 (for carboxypeptidase A (CPA)) at 37°C. Changes in absorbance at 405 nm were measured as described previously (36).

Culture of primary and maturated BMMCs

Bone marrow cells were obtained from the femurs and tibias of mice and cultured in IL-3-containing BMMC-complete medium comprising DMEM, 10% FBS, 2 mM L-glutamine, 100 IU/ml penicillin, 100 • g/ml streptomycin, 100 mM nonessential amino acids, and 5 ng/ml mouse rIL-3. Nonadherent cells were transferred to fresh IL-3-containing BMMC-complete medium at least once a week. After 4–5 wk of culture, the majority of the floating cells were confirmed to be immature mast cells as assessed by Alcian blue-positive and safranin-negative staining of their granules.

The maturation of immature BMMCs toward CTMC-like cells was described previously in detail (14). Briefly, 5 • 10^6 BMMCs were seeded on the subconfluent Swiss 3T3 fibroblast monolayer in 100-mm culture dishes and cocultured for 4–6 days in the presence of 50 ng/ml SCF with replacement of the medium every 2 days. The cells were trypsinized and replated, and nonadherent cells (• 95% were mast cells) were collected and used for analyses. The maturation of BMMCs into CTMC-like cells was verified by staining of their granules with Alcian blue and counterstaining with safranin O.

Western blotting

BMMCs (10^5) were lysed in SDS-PAGE sample buffer (63 mM Tris-HCl (pH 6.8), 2% SDS, 10% glycerol, and 0.08% bromophenol blue) containing 5% 2-ME and subjected to SDS-PAGE. Proteins were subsequently blotted onto nitrocellulose membranes, followed by blocking with 5% milk powder in PBS containing 0.05% Tween 20. The membranes were incubated for 1 h with rabbit anti-mouse NDRG1 polyclonal Ab (15) followed by reprobing with mouse anti-• -tubulin mAb (Zymed Laboratories) at 1/5000 dilution in PBS with 0.05% Tween 20. Tyrosine phosphorylation of phospholipase C (PLC) •1 and •2 was determined by immunoblotting with rabbit anti-human phospho-PLC•1 (Tyr^{783}) and •2 (Tyr^{1217}) polyclonal Abs followed by reprobing with rabbit anti-human PLC•1 and •2 polyclonal Abs (Cell Signaling Technology) at 1/1000 dilution in PBS with 0.05% Tween 20 (37). After washing with PBS and 0.05% Tween 20, the membranes were incubated with a secondary anti-rabbit Ig Ab conjugated with HRP (Zymed) at 1/5000 dilution in PBS plus 0.05% Tween 20. After 1 h of incubation the membranes were washed extensively with PBS plus 0.05% Tween 20 followed by washing with PBS without detergent. The membranes were developed with the ECL system (PerkinElmer Life Sciences) according to the protocol provided by the manufacturer.

RT-PCR

Total RNA was extracted from BMMCs with TRIzol reagent (Invitrogen Life Technologies). First-strand cDNA synthesis was conducted using the SuperScript III reverse transcriptase kit (Invitrogen Life Technologies). Five micrograms of total RNA was used in reactions primed with oligo(dT) (12–18-mer) primer (Invitrogen Life Technologies) to obtain cDNA. Then, 1 • l of the synthesized cDNA was used as the template for the mRNA amplification reactions. The PCR amplification was performed using a GeneAmp PCR System 9600 (PerkinElmer) using a standard PCR protocol. The RT-PCR product was analyzed on a 1.5% agarose gel and visualized using ethidium bromide staining.

The primer pairs for NDRG1, NDRG2, NDRG3, and NDRG4 were described previously (32). The primer pairs were 5•-ACCACATTCTCGC CCTTACAT-3• and 5•-TCTCAGTTTCACCTCCCTCAG-3• for mouse mast cell protease (mMCP)-4; 5•-ATAACAGTCCTCCTAGGAGCC-3• and 5•-GATCCAGGGCCTGTAATGGGA-3• for mMCP-5; 5•-GCACA TCAAAAGCCCACAGC-3• and 5•-TAGACAGGGGAGACAGAGGA C-3• for mMCP-6; 5•-CAGGCAGGCACAGTTATGCAA-3• and 5•-A ACCCAGTCTAAGGAAGACC-3• for mMC-CPA3; 5•-ATGGAGACC CCATTGCTCTGA-3• and 5•-ATGATCTCCATTGAGGCTGCC-3• for N-deacetylase/N-sulfotransferase-2; 5•-CAGCTAGTTGTCAATCCTGCTCT TC-3• and 5•-GGTGCAGCTTATCGATGAATCCAG-3• for IL-4; 5•-CAG AGGATACCACTCCCAACAGAC-3• and 5•-CCTTAGCCACTCCTTCTG TGACTC-3• for IL-6; 5•-GAAAGCATGATCCGCGACGTGGAA-3• and 5•-GCTGACGGTGTGGGTGAGGAGCAC-3• for TNF-•; and 5•-TCGTGGA TCTGACGTGCCGCCTG-3• and 5•-CACCACCCTGTTGCTGTAGCCGT AT-3• for GAPDH.

Flow cytometry

Suspensions of 10^6 BMMCs were treated with rat anti-mouse CD16/CD32 (Fc•RII/RIII) mAb (clone 2.4G2, BD Biosciences Pharmingen) (final concentration, 10 • g/ml) in 2% FBS-PBS for 10 min on ice to block cell surface Fc•Rs, followed by incubation for 45 min with FITC-labeled rat anti-mouse CD117 (c-kit) mAb (clone 2B8, BD Biosciences) at 1/50 dilution in the same buffer. To assess Fc•RI expression, the cells were treated for 3 h with 10 • g/ml mouse IgE (SPE-7). Fc•Rs were blocked as described above and the cells were subsequently incubated with PE-labeled rat anti-mouse IgE mAb (clone 23G3; eBioscience) at 1/50 dilution in 2% FBS-PBS. Flow cytometry was conducted on a FACSCalibur instrument (BD Biosciences).

Activation of BMMCs

For stimulation with IgE plus polyvalent Ag (DNP-BSA), BMMCs (10^7 cells/ml) before and after coculture with fibroblasts were sensitized with 100 ng/ml anti-DNP IgE for 1 h at 37°C. After washing with medium, the cells were stimulated for appropriate periods with various doses of DNP-BSA at 37°C. For stimulation with compound 48/80, the cells were treated for the appropriate periods with various doses of compound 48/80 at 37°C. The resulting supernatants and cell pellets were then taken for a •-HEX assay. The cysteinyl leukotriene (LT) C_4 (LTC_4) production was determined using enzyme immunoassay kits according to the manufacturer's instructions (Cayman Chemical). Replicate cells were subjected to RNA extraction followed by RT-PCR for several cytokines, as noted above.

Statistical analysis

Results from in vivo and ex vivo experiments (mean • SEM) were assessed with Student's unpaired, two-tailed t test. Differences between replicate $Ndrg1^{+/+}$ and $Ndrg1^{-/-}$ groups were regarded as significant at p • 0.05, unless otherwise stated.

Results

Impaired mast cell-associated anaphylactic reactions in Ndrg1-deficient mice

Anaphylaxis represents an extreme form of mast cell-associated allergic reaction consisting of a sensitization phase in which allergen-specific IgE is produced and binds to mast cell surfaces and a subsequent acute effector phase in which allergen-induced activation of mast cells leads to the release of copious amounts of vasoactive amines and other inflammatory mediators (38). To clarify the in vivo role of NDRG1 in mast cell biology, we first examined the mast cell-dependent, IgE-mediated passive systemic anaphylactic reaction in Ndrg1-deficient mice.

$Ndrg1^{+/+}$ and $Ndrg1^{-/-}$ mice were sensitized with IgE directed against DNP and challenged 24 h later with DNP-HSA as an Ag, and their rectal temperatures were monitored at regular intervals. As shown in Fig. 1A, a temporary decrease in rectal temperature was observed in $Ndrg1^{+/+}$ mice 10–20 min after antigenic challenge, whereas such a decrease was virtually absent from mast cell-deficient W/W^v mice. Notably, although a significant decrease in rectal temperature following antigenic challenge was observed in $Ndrg1^{+/+}$ mice, it was modest in comparison with that in $Ndrg1^{-/-}$ mice. Serum samples were taken from these mice 1.5 min after Ag challenge for the determination of histamine concentration. As shown in Fig. 1B, $Ndrg1^{+/+}$ mice showed a marked increase in the serum histamine level upon the cross-linking of Fc•RI, whereas no appreciable increase was evident in W/W^v mice. Although there was a significant increase of the serum histamine level in Ag-challenged $Ndrg1^{-/-}$ mice compared with that in W/W^v mice, it reached a mean value of only 37% relative to that in replicate $Ndrg1^{+/+}$ mice (21.1 • 1.6 vs 7.9 • 1.6 nM in $Ndrg1^{+/+}$ and $Ndrg1^{-/-}$ mice, respectively; p • 0.01, n • 11).

To further assess the role of NDRG1 in anaphylaxis, we next investigated the capacity of Ndrg1-deficient mice to respond to immune challenge in PCA, where local extravasation and tissue swelling are induced by the local application of Ag-specific IgE followed by i.v. challenge of Ag. The ears of $Ndrg1^{+/+}$ and $Ndrg^{-/-}$ mice were injected intradermally with DNP-specific IgE and challenged 24 h later with an i.v. injection of DNP-HSA together with Evans blue dye. Mediators released upon mast cell activation increase vascular permeability, which allows the dye to leak from blood vessels into the surrounding tissue, causing edema and providing a measure of mast cell activation.

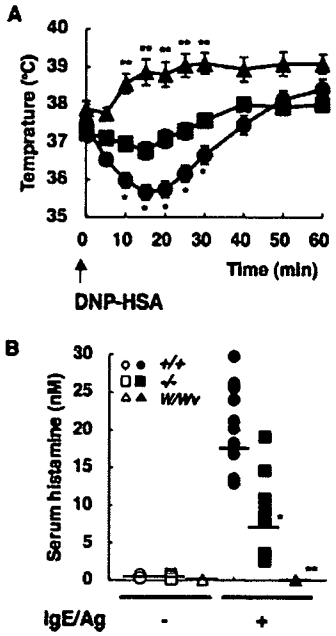

FIGURE 1. Effects of NDRG1 deficiency on IgE-mediated, Ag-dependent passive systemic anaphylaxis as assessed by rectal temperature change and serum histamine concentration. A, Ndrg1$^{+/+}$ (circles; n • 13), Ndrg1$^{-/-}$ (squares; n • 13), and WBB6F$_1$-W/W^v (W/W^v, triangles; n • 3) mice were sensitized with anti-DNP IgE and challenged with DNP-HSA to induce systemic anaphylaxis as described in Materials and Methods. Passive systemic anaphylactic response was monitored by measuring rectal temperatures at the indicated times after antigenic challenge. B, The histamine concentrations in sera from individual Ndrg1$^{+/+}$ (• /• , n • 11), Ndrg1$^{-/-}$ (• /• , n • 11), and WBB6F$_1$-W/W^v (W/W^v, n • 3) mice after Ag challenge for 30 min (filled symbols) or no stimulation (open symbols) were plotted, with the mean value for each group indicated by a line. •, p • 0.01 vs Ndrg1$^{-/-}$; and ••, p • 0.01 vs Ndrg1$^{-/-}$ mice.

As shown in Fig. 2A, marked extravasation of Evans blue was seen in the ears of Ndrg1$^{-/-}$ mice 30 min after Ag challenge, whereas the ears of replicate Ndrg1$^{+/+}$ mice exhibited markedly less extravasation of the dye. Consistently, when tissue swelling of the left and right ears was measured with a dial thickness gauge, the change in ear thickness of Ndrg1$^{-/-}$ mice was as little as 40% compared with that of Ndrg1$^{+/+}$ mice (61.7 • 6.7 vs 24.7 • 4.3 • m in Ndrg1$^{-/-}$ and Ndrg1$^{+/+}$ mice, respectively; p • 0.01, n • 15) (Fig. 2B). To evaluate the extravasation of Evans blue quantitatively, the ears were removed and the OD of the extracted dye was measured as a function of Ag dose (Fig. 2C) or time (Fig. 2D). We observed that Evans blue extravasation was lower in Ndrg1$^{-/-}$ mice than in replicate Ndrg1$^{+/+}$ mice at all Ag doses (Fig. 2C) and all time points (Fig. 2D), even though dye extravasation was still evident in Ndrg1$^{-/-}$ mice. Furthermore, when these mice were intradermally administered compound 48/80, a polycationic IgE-independent mast cell secretogogue, a result similar to the IgE-associated passive immune response was obtained. Thus, the extravasation of Evans blue was only modest in Ndrg1$^{-/-}$ mice treated with compound 48/80 relative to that in replicate Ndrg1$^{+/+}$ mice (Fig. 2E). In mast cell-deficient W/W^v mice there was minimal dye extravasation under all conditions tested (Fig. 2, B–E). Collectively, these results indicate that NDRG1 deficiency causes a significant reduction of mast cell-associated passive systemic and local cutaneous anaphylactic reactions.

Histochemical and functional analyses of mast cells in Ndrg1-deficient mice

Because NDRG1 is widely expressed in many tissues/cells, it was still not apparent whether the diminished anaphylaxis reactions

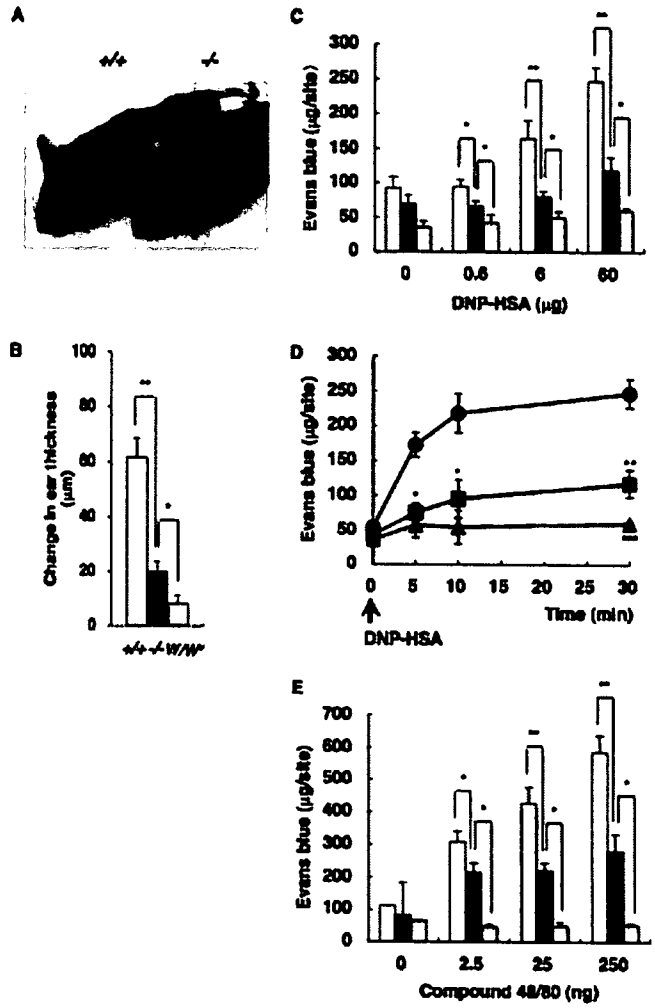

FIGURE 2. Effects of NDRG1 deficiency on PCA as assessed by ear swelling and Evans blue extravasation. Ndrg1$^{+/+}$ (• /•), Ndrg1$^{-/-}$ (• /•), and WBB6F$_1$-W/W^v (W/W^v) mice were sensitized with anti-DNP IgE and challenged 24 h later with DNP-HSA (A–D) or directly treated with compound 48/80 (E) together with Evans blue to induce PCA as described in Materials and Methods. A, Dye extravasation following administration of 60 • g of Ag was visualized by blue staining at the injection sites in the ears of Ndrg1$^{+/+}$ and Ndrg1$^{-/-}$ mice. Photographs of the mice were taken 30 min after Ag challenge. One representative of 11 mice for each genotype is shown. B, Ear thickness of Ndrg1$^{+/+}$ (n • 15), Ndrg1$^{-/-}$ (n • 15), and W/W^v (n • 6) mice was measured before and 30 min after Ag challenge using a dial thickness gauge. Ear thickness change, which represents the degree of ear swelling, was determined as the difference before and after Ag challenge into the right and left ears of each mouse. ••, p • 0.01; and •, p • 0.05. C, Dose-dependent extravasation of Evans blue into the ears of mice following IgE-mediated, Ag-dependent PCA. Ears of the IgE-sensitized Ndrg1$^{+/+}$ (open bars), Ndrg1$^{-/-}$ (filled bars), and W/W^v (gray bars) mice were challenged with 0 (n • 3), 0.6 (n • 9), 6 (n • 10), and 60 (n • 18) • g of DNP-HSA for 30 min. Extravasation of Evans blue was quantified as described in Materials and Methods. ••, p • 0.01 and •, p • 0.05. D, Kinetics of extravasation of Evans blue into the ears of mice following IgE-mediated, Ag-dependent PCA. Ears of the IgE-sensitized Ndrg1$^{+/+}$ (circles, n • 18, respectively), Ndrg1$^{-/-}$ (squares; n • 13, respectively), and W/W^v (triangles; n • 4, respectively) mice were challenged with 60 • g of DNP-HSA for the indicated periods. •, p • 0.01; and ••, p • 0.05 vs Ndrg1$^{-/-}$ mice. •••, p • 0.05 vs Ndrg1$^{-/-}$ mice. E, Dose-dependent extravasation of Evans blue into the ears of mice following compound 48/80-induced PCA. The left and right ears of Ndrg1$^{+/+}$ (open bars), Ndrg1$^{-/-}$ (filled bars), and W/W^v (gray bars) mice were treated with 0 (n • 3), 2.5 (n • 10), 25 (n • 10), and 250 (n • 10) ng of compound 48/80 for 30 min. ••, p • 0.01, and •, p • 0.05.

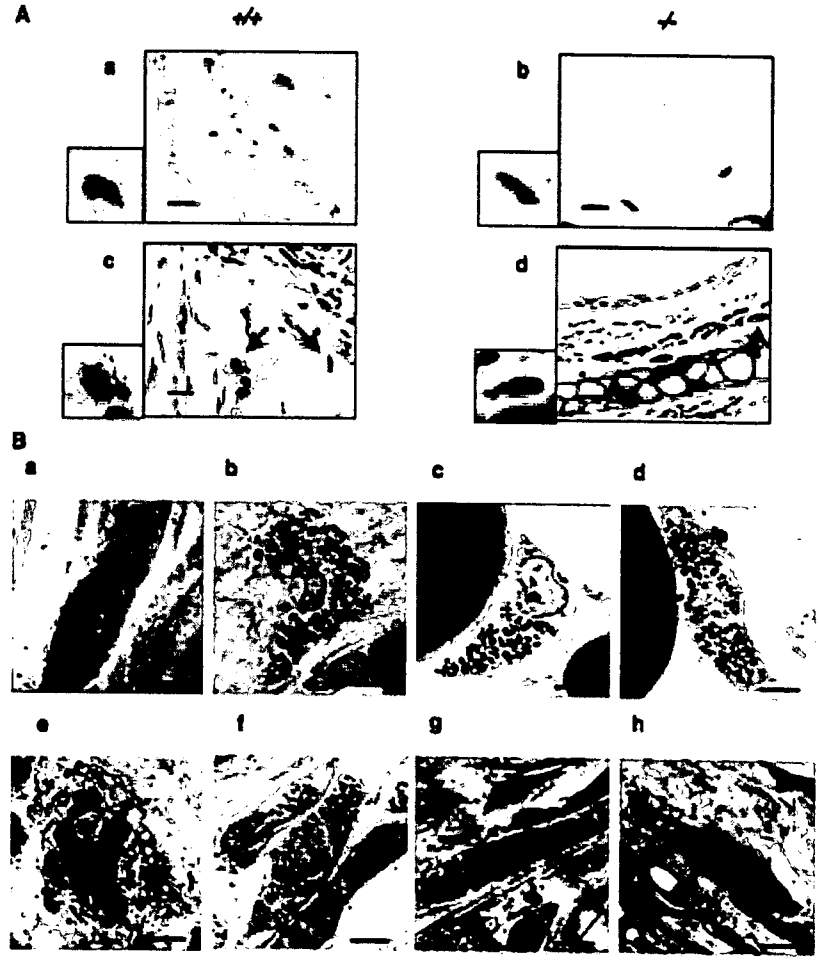

FIGURE 3. Histological and ultrastructural features of mast cells in the ear skin of wild-type and Ndrg1-deficient mice before and after Ag challenge. A, Ndrg1$^{+/+}$ (+/+) and Ndrg1$^{-/-}$ (-/-) mice were subjected to IgE-mediated, Ag-dependent PCA as described in Materials and Methods. Before and 2 min after Ag challenge the ear sections were stained with toluidine blue and examined by light microscopy. Photographs of Ndrg1$^{+/+}$ (a and c) and Ndrg1$^{-/-}$ (b and d) tissue sections before (a and b; n = 20 for each) and after (c and d; n = 10 for each) Ag challenge are shown. Yellow and red arrows indicate intact and degranulated tissue mast cells, respectively. Black arrows indicate chromocytes. Magnified views of a single mast cell for each are shown in the insets (a–d). Bar, 10 μm. B, Transmission electron microscopy (lead citrate staining) of ear skin mast cells in Ndrg1$^{+/+}$ (a, b, and e) and Ndrg1$^{-/-}$ (c, d, and f–h) mice before (a–d) and after (e–h) Ag challenge. Bar, 2 μm.

could be due to a defect in mast cells or other cell types, such as endothelial cells (39). To investigate the underlying mechanism(s) responsible for the reduced allergic reactions in Ndrg1-deficient mice, we next examined mast cells in the ear skin of wild-type and Ndrg1-deficient mice histochemically during the IgE-mediated, Ag-dependent PCA. Ear sections of Ndrg1$^{+/+}$ and Ndrg1$^{-/-}$ mice with or without Ag challenge were stained with toluidine blue to quantify degranulated tissue mast cells by light microscopy. In the absence of Ag challenge (no stimulation), the ear skin of Ndrg1$^{-/-}$ mice contained 37.8% fewer intact toluidine blue-positive mast cells than that of Ndrg1$^{+/+}$ mice (Fig. 3A, a and b, and Table I). After challenge with Ag for 2 min, the ear skin sections of Ndrg1$^{+/+}$ and Ndrg1$^{-/-}$ mice contained 18.8 and 2.8% degranulated mast cells relative to their respective total mast cells, revealing ~ 85% less degranulation in the null mice than in the control mice (Fig. 3A, c and d, and Table I). These observations suggest that the number of ear skin mast cells is reduced and that the degranulation efficacy of these cells is markedly impaired as a result of NDRG1 deficiency.

Table I. Quantification of ear skin mast cells in Ndrg1$^{+/+}$ and Ndrg1$^{-/-}$ mice[a]

	IgE/Ag	Intact	Degranulated
Ndrg1$^{+/+}$	No stimulation	660.7 ± 52.7	9.7 ± 2.0 (1.5%)
	Two minutes	930.0 ± 76.7	175.0 ± 10.8 (18.8%)
Ndrg1$^{-/-}$	No stimulation	411.3 ± 39.3*	4.4 ± 4.6* (1.0%)
	Two minutes	720.0 ± 50.4*	20.0 ± 6.6* (2.8%)

[a] Activation of skin mast cells (per mm^2) with or without Ag application was evaluated by counting the numbers of intact and degranulated toluidine blue-positive cells in 20 different ear sections from Ndrg1$^{+/+}$ (n = 5) and Ndrg1$^{-/-}$ (n = 5) mice by light microscopy. The results are expressed as mean ± SEM.

*, $p < 0.01$ vs Ndrg1$^{+/+}$ mice under each condition; percentages of degranulated mast cells relative to total mast cells are shown in parentheses.

To further corroborate the abnormal histochemical aspects of ear skin mast cells, we next examined their ultrastructural features by transmission electron microscopy after 2 min of stimulation with Ag in comparison with those of unstimulated cells. As shown in Fig. 3B, there were obvious and significant differences in secretory granule and cell surface morphology between Ndrg1$^{+/+}$ and Ndrg1$^{-/-}$ ear mast cells. Intact mast cells in Ndrg1$^{+/+}$ mice were oval with regular short processes and had many secretory granules filled with electron-lucent and dense contents (Fig. 3B, a and b). Relative to the mast cells in Ndrg1$^{+/+}$ mice, those in Ndrg1$^{-/-}$ mice had unusual granules that were small and irregular in size (Fig. 3B, c and d), suggesting immaturity. Two minutes after antigenic challenge the ear skin mast cells in Ndrg1$^{+/+}$ mice possessed swollen granules that exhibited a loss of crystalline materials and decreased electron density (Fig. 3Be). The fusion of swollen granules had resulted in the formation of large vacuolar degranulation channels continuous with the plasma membrane and, thereby, the appearance of large surface pores. Massive exocytosis, demonstrated by the extrusion of flocculent matrix materials through the surface pores into the extracellular space, was regularly observed in Ndrg1$^{+/+}$ mast cells (Fig. 3Be). In contrast, these Ag-induced morphological changes were scarcely observed in Ndrg1$^{-/-}$ mast cells (Fig. 3B, f, g, and h). Thus, it is likely that the reduced PCA response in Ndrg1-deficient mice (Fig. 2) resulted from abnormalities in the maturation and exocytosis of mast cells in the ear skin.

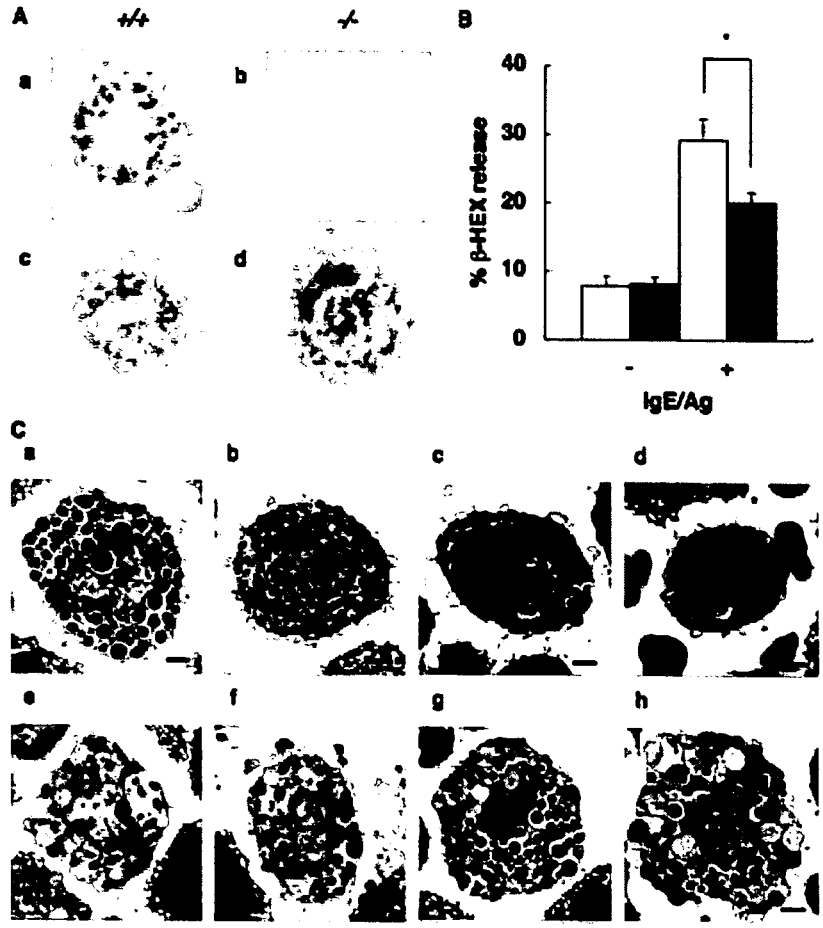

FIGURE 4. Morphology and exocytotic response of PMCs from wild-type and Ndrg1-deficient mice. A, Immunohistochemistry of NDRG1 in PMCs from Ndrg1$^{+/+}$ (a, • /•) and Ndrg1$^{-/-}$ (b, • /•) mice. In each case the cells were incubated with an anti-NDRG1 Ab and then with a HRP-conjugated anti-goat Ig. Other sets of PMC preparations from Ndrg1$^{+/+}$ (c) and Ndrg1$^{-/-}$ (d) mice were stained with safranin O. Representative data from five independent experiments are shown. B, The exocytotic response was determined by measuring the release of •-HEX. PMCs (10^6) from Ndrg1$^{+/+}$ (open bars) and Ndrg1$^{-/-}$ (filled bars) mice were sensitized with anti-DNP IgE and stimulated with DNP-BSA plus lyso-PS as described in Materials and Methods. •-HEX enzymatic activity (n • 6) was measured in supernatants and cell pellets solubilized with 0.5% Triton-X-100 in PIPES-buffered saline. •, p • 0.01. C, Transmission electron microscopy of PMCs prepared from Ndrg1$^{+/+}$ (a, b, e, and f) and Ndrg1$^{-/-}$ (c, d, g, and h) mice before (a–d) and after (e–h) exo vivo stimulation. Bar, 1 • m.

We then examined the morphology and ex vivo function of PMCs isolated from wild-type and Ndrg1-deficient mice. The immunostaining of cytospun PMCs with the anti-NDRG1 Ab showed intense immunoreactivity in Ndrg1$^{+/+}$ but not Ndrg1$^{-/-}$ PMCs (Fig. 4A, a and b), confirming the specificity of the Ab. Interestingly, NDRG1 immunoreactivity in Ndrg1$^{+/+}$ PMCs was largely associated with compact granular structures (Fig. 4Aa), a staining pattern similar to that of replicate cells treated with safranin O (Fig. 4Ac), which stains heparin-containing serglycin proteoglycan in secretory granules. Considering that NDRG1 is a cytosolic protein, this result may indicate that NDRG1 is located in close contact with the cytosolic surface of secretory granules. The fact that the granules in Ndrg1$^{+/+}$ and Ndrg1$^{-/-}$ PMCs were equally safranin-positive (Fig. 4A, c and d) suggests that NDRG1 deficiency does not affect heparin synthesis. Notably, safranin staining of cytospin preparations of peritoneal cells demonstrated that Ndrg1$^{-/-}$ mice contained 53.4% fewer safranin-positive PMCs than Ndrg1$^{+/+}$ mice (4885 • 492 vs 2280 • 225 per 10^6 peritoneal cells in Ndrg1$^{+/+}$ and Ndrg1$^{-/-}$ mice, respectively (p • 0.01), in 15 independent cytospin preparations). Hence, Ndrg1-deficient mice contain significantly less CTMC-type mast cells (both in the ear (Fig. 3) and the peritoneum (Fig. 4)) than do wild-type mice. We then compared IgE/Ag-dependent degranulation of PMCs from Ndrg1$^{+/+}$ and Ndrg1$^{-/-}$ mice by measuring the release level of the extracellular activity of •-HEX, a marker enzyme for histamine-containing granules. Because IgE/Ag-dependent activation of rodent PMCs is greatly augmented by lyso-PS (40–42), PMCs sensitized with anti-DNP IgE were stimulated by Fc•RI cross-linking with DNP-BSA as an Ag in the presence of lyso-PS as a cofactor. As shown in Fig. 4B, PMCs from Ndrg1$^{-/-}$ mice displayed significantly less release of •-HEX than those from Ndrg1$^{+/+}$ mice in response to IgE/Ag plus lyso-PS, whereas the basal release levels of these mediators were indistinguishable between the two genotypes.

Ultrastructural analyses under electron microscopy revealed that Ndrg1$^{-/-}$ mice contained a population of PMCs that looked similar to Ndrg1$^{+/+}$ PMCs (Fig. 4C, a and b for Ndrg1$^{+/+}$ and c for Ndrg1$^{-/-}$) and another population with fewer and irregular granules (Fig. 4Cd). After IgE/Ag (plus lyso-PS) stimulation, Ndrg1$^{+/+}$ PMCs were well degranulated (Fig. 4C, e and f), whereas a large portion of intact granules still remained in Ndrg1$^{-/-}$ PMCs (Fig. 4C, g and h). Thus, these functional and morphological studies imply that NDRG1 deficiency causes a reduced Fc•RI-mediated exocytotic response of CTMCs both in vivo (skin mast cells; Fig. 3) and ex vivo (PMCs; Fig. 4).

To further assess the differences in secretory granules between Ndrg1$^{+/+}$ and Ndrg1$^{-/-}$ mast cells, we measured the content of histamine and the activity of mast cell-associated proteases in homogenates of ears or peritoneal cells from both genotypes. Histamine levels and chymase-, typtase-, and CPA-like protease activities were pretty low in the ears (Fig. 5, Aa and B, a–c) and peritoneal cells (Fig. 5Ab) of mast cell-deficient W/W^v mice, confirming that mast cells are the main source of these granule components. As shown in Fig. 5A, histamine levels in the ears (a) and peritoneal cells (b) of Ndrg1$^{+/+}$ and Ndrg1$^{-/-}$ mice were comparable. Given that the number of mast cells was decreased by half in both ears and peritoneal cavities by Ndrg1 deficiency (see above), histamine content per PMC was estimated to nearly double in Ndrg1$^{-/-}$ over Ndrg1$^{+/+}$ mice (Fig. 5A, c and d). Measurement of chymase-like (Fig. 5Ba), tryptase-like (Fig. 5Bb), and CPA (Fig. 5Bc) activities in the ears showed that the tryptase-like, but not chymase-like and CPA, activity was significantly reduced in

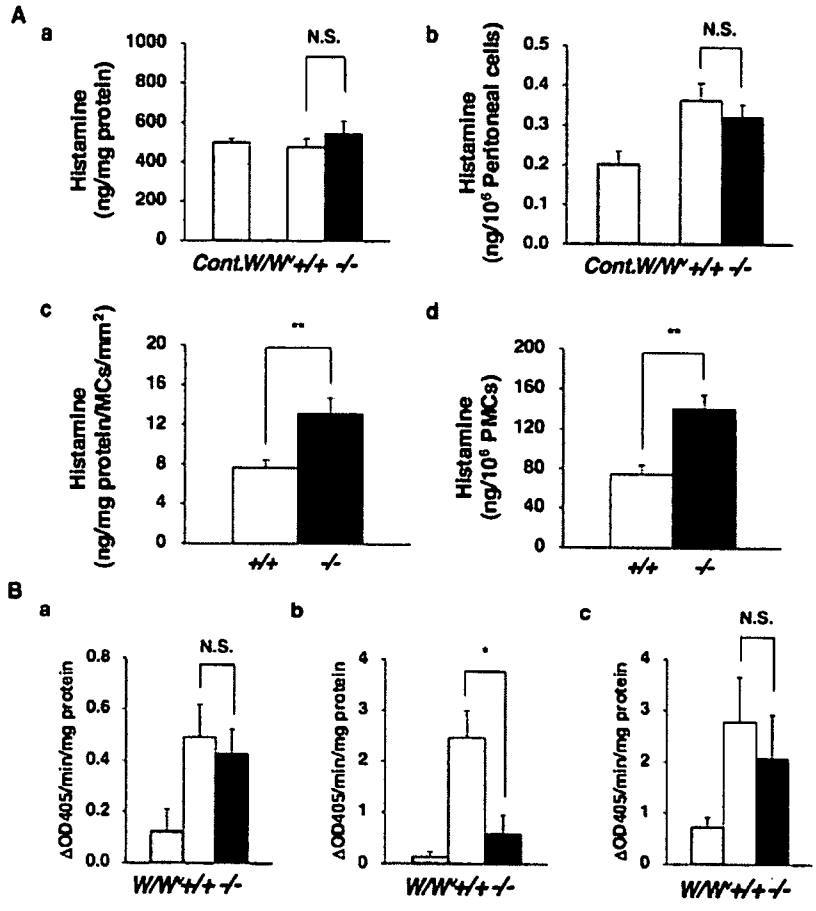

FIGURE 5. The storage of granule histamine and proteases in tissue mast cells of wild-type and Ndrg1-deficient mice. A, The histamine contents in ear extracts (a and c) and peritoneal cells (b and d) from Ndrg1$^{+/+}$ ($^{+/+}$, n • 13), Ndrg1$^{-/-}$ ($^{-/-}$, n • 12), control WBB6F$_1$-$^{+/+}$ (Cont.W, n • 3), and WBB6F$_1$-W/W^v (W^v, n • 3) mice. Data were shown as histamine (ng) per protein of ear tissue (a) or 10^6 peritoneal cells (b) and per protein of ear skin mast cells per mm^2 (c) or 10^6 PMCs (d). ••, p • 0.01; and N.S., not significant. B, Protease activities in ear tissue extracts from Ndrg1$^{+/+}$ (n • 7), Ndrg1$^{-/-}$ (n • 8), and W/W^v (n • 5) mice. The extracts prepared from ear tissue were assayed for trypsin-like (a), chymotrypsin-like (b), and CPA (c) activities as described in Materials and Methods. Data were shown as protease activities per protein of ear tissue. •, p • 0.05; and N.S., not significant.

Ndrg1$^{-/-}$ mice compared with that in Ndrg1$^{+/+}$ mice. These results suggest that the absence of Ndrg1 alters the features of secretory granules in CTMCs.

Impaired maturation and reduced exocytotic degranulation of BMMCs derived from Ndrg1-deficient mice

To further evaluate the abnormal aspects of mast cells observed in Ndrg1-deficient mice, we analyzed BMMCs of Ndrg1$^{+/+}$ and Ndrg1$^{-/-}$ mice that were obtained after bone marrow cells were cultured for 4–5 wk in IL-3-containing medium. Nearly 95% of the cells in these cultures from both genotypes were mast cells, as they contained metachromatic granules after staining with Alcian blue (Fig. 6A, a and e) or toluidine blue (data not shown). The kinetics of cell growth and the expression of mast cell surface markers (c-kit$^+$ CD34$^+$ or c-kit$^+$ Sca-1$^+$ as determined by flow cytometric analysis) were also similar between the BMMCs from both sources (data not shown). Electron microscopy studies of various preparations of BMMCs from Ndrg1$^{+/+}$ and Ndrg1$^{-/-}$ mice revealed similar cell morphology and membrane projections and the presence of morphologically distinct cytoplasmic granules, including those with internal vacuoles (type I), those with an electron-dense core surrounded by membrane vacuoles (type II), and those completely filled with the electron-dense core (type III) (Fig. 6A, c and g) (43). These results indicate that NDRG1 is not essential for IL-3-dependent development of BMMCs from bone marrow progenitor cells.

We next examined whether the loss of NDRG1 would have some impact on the maturation of immature BMMCs toward CTMC-like mast cells. As reported previously, a coculture of BMMCs with Swiss 3T3 fibroblasts in the presence of SCF facilitates morphological and functional maturation toward a CTMC-like phenotype (14), and NDRG1 is an early inducible protein in this process (15). Therefore, as expected, NDRG1 protein was minimally expressed before coculture and was markedly induced after coculture in Ndrg1$^{+/+}$ BMMCs, whereas it was undetectable in Ndrg1$^{-/-}$ BMMCs irrespective of coculture (Fig. 6B). When Ndrg1$^{+/+}$ and Ndrg1$^{-/-}$ BMMCs after coculture with fibroblasts were counterstained with safranin O, the latter appeared less granulated than the former (Fig. 6A, b and f). Indeed, electron microscopy showed that, in contrast with cocultured Ndrg1$^{+/+}$ BMMCs in which type III secretory granules were well organized (Fig. 6Ad), replicate Ndrg1$^{-/-}$ BMMCs had mainly type I and type II secretory granules that were small and irregular in size and were partially unfilled with electron-lucent and dense contents (Fig. 6Ah). Moreover, the number of Ndrg1$^{+/+}$ BMMCs increased • 3-fold after 4 days of coculture, whereas replicate Ndrg1$^{-/-}$ BMMCs grew slower (2.9 • 0.2 vs 2.2 • 0.1 -fold for Ndrg1$^{+/+}$ and Ndrg1$^{-/-}$ BMMCs, respectively; p • 0.01; n • 13), suggesting that Ndrg1 deficiency has a propensity to reduce the expansion of mast cells interacting with fibroblasts.

We next performed RT-PCR using RNA samples from BMMCs of Ndrg1$^{+/+}$ and Ndrg1$^{-/-}$ mice to compare the expression patterns of all NDRG members. Consistent with our previous report (15), NDRG1 mRNA was weakly expressed before coculture and was highly induced as early as 1 h after the start of coculture in wild-type BMMCs, whereas it was not detected at all in Ndrg1-deficient BMMCs (Fig. 6C). We found that NDRG2, NDRG3, and NDRG4 mRNAs were also expressed in both Ndrg1$^{+/+}$ and Ndrg1$^{-/-}$ BMMCs (Fig. 6C). In contrast to the marked inducibility of NDRG1, expressions of NDRG2, NDRG3, and NDRG4 were nearly constant throughout the experimental period. Judging from the optimized PCR cycles, the expression level of NDRG1 was • 30-fold higher than that of NDRG3 and

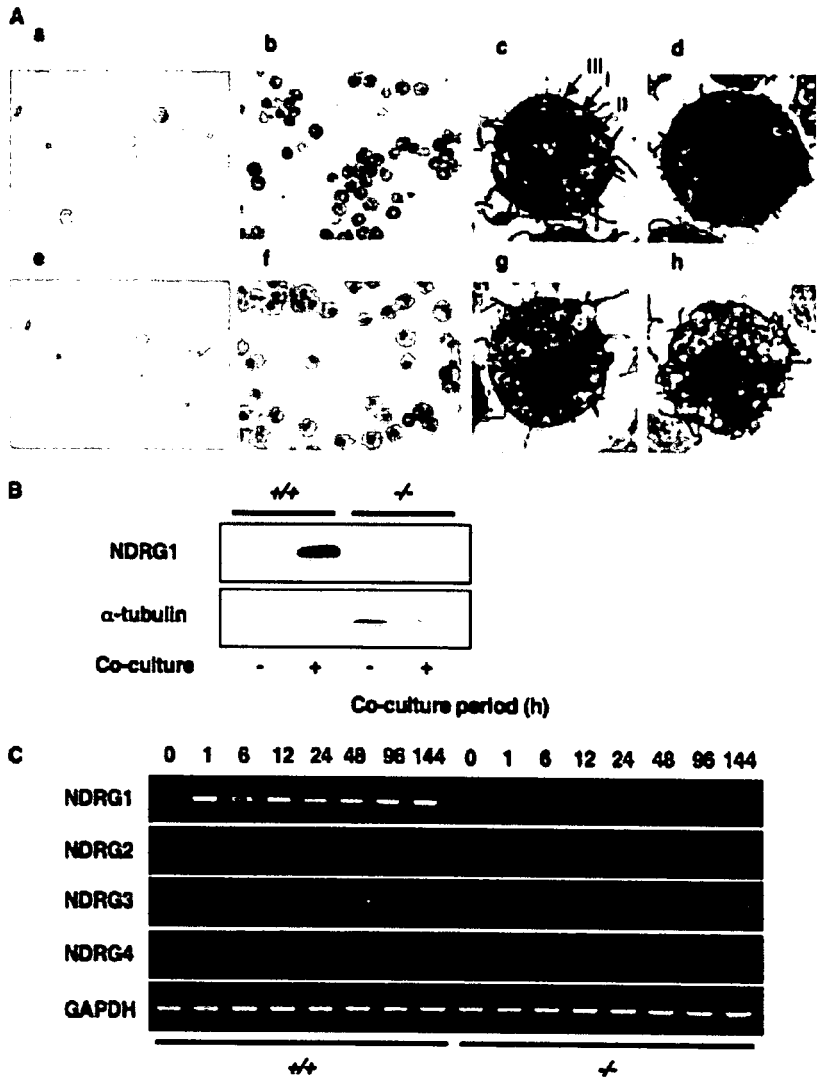

FIGURE 6. Histological and ultrastructural features of wild-type and Ndrg1-deficient BMMCs before and after coculture with fibroblasts. A, The cytospin preparations of Ndrg1$^{+/+}$ (a and b) and Ndrg1$^{-/-}$ (e and f) BMMCs before (a and e) and after (b and f) coculture with fibroblasts in the presence of SCF were stained by Alcian blue and safranin O. Ndrg1$^{+/+}$ (c and d) and Ndrg1$^{-/-}$ (g and h) BMMCs before (c and g) and after (d and h) coculture with fibroblasts were further analyzed by electron microscopy to reveal their ultrastructures. Typical types I, II, and III granules in BMMCs are shown by arrows. B, Expression of NDRG1 protein in Ndrg1$^{+/+}$ (+/+) and Ndrg1$^{-/-}$ (-/-) BMMCs before and after coculture with fibroblasts as assessed by Western blotting with anti-NDRG1 Ab. Blotting with β-tubulin was also performed to confirm the equal sample loading. Representative results for BMMCs from Ndrg1$^{+/+}$ and Ndrg1$^{-/-}$ mice are shown. C, mRNA expression of NDRG family members. RT-PCR analysis was performed on total RNA samples from Ndrg1$^{+/+}$ and Ndrg1$^{-/-}$ BMMCs before and after coculture for the indicated periods to detect transcripts for NDRG1 (23 cycles of amplification), NDRG2 (32 cycles), NDRG3 (28 cycles), and NDRG4 (35 cycles). Expression of GAPDH was examined as an internal control (23 cycles).

even more than that of NDRG2 and NDRG4 in wild-type BMMCs after coculture.

Next, we compared the granule release from Ndrg1$^{+/+}$ and Ndrg1$^{-/-}$ BMMCs before and after coculture with fibroblasts by measuring the extracellular activity of β-HEX. BMMCs were incubated with DNP-specific IgE and subsequently stimulated by Fcε RI cross-linking with DNP-BSA. In dose-related (Fig. 7, A and C) and kinetic (Fig. 7, B and D) granule release responses, Ndrg1$^{-/-}$ BMMCs after coculture displayed significantly less exocytosis than did replicate Ndrg1$^{+/+}$ BMMCs (Fig. 7, C and D), whereas the responses of IL-3-maintained immature BMMCs derived from both genotypes were comparable (Fig. 7, A and B). It was noteworthy that Ndrg1$^{-/-}$ BMMCs after coculture released more β-HEX than before coculture, whereas this increased exocytosis after coculture was almost absent from Ndrg1$^{+/+}$ BMMCs. The total amount of β-HEX per cell did not differ between Ndrg1$^{+/+}$ and Ndrg1$^{-/-}$ BMMCs before and after coculture, and treatment with IgE alone did not induce granule release from either genotype (data not shown).

Because the coculture of BMMCs with fibroblasts led to the acquisition of responsiveness to compound 48/80 (14), we next compared the responses of Ndrg1$^{+/+}$ and Ndrg1$^{-/-}$ BMMCs to this G_i-coupled polycationic secretagogue after coculture with fibroblasts. The stimulation of cocultured Ndrg1$^{+/+}$ BMMCs with compound 48/80 resulted in marked exocytosis, whereas that of replicate Ndrg1$^{+/+}$ BMMCs provided partial albeit significant (~ 50% reduction as compared with Ndrg1$^{+/+}$ BMMCs) responses at all doses (Fig. 7E) and times (Fig. 7F) tested. Furthermore, β-HEX release in response to the Ca^{2+} ionophore (ionomycin) was also substantially reduced in Ndrg1$^{-/-}$ BMMCs relative to Ndrg1$^{+/+}$ BMMCs after coculture (61.0 and 41.7% release in Ndrg1$^{+/+}$ and Ndrg1$^{-/-}$ BMMCs, respectively, at 1 μM ionomycin). Collectively, these observations suggest that Ndrg1-deficient BMMCs after coculture with fibroblasts in the presence of SCF are functionally less mature than replicate wild-type BMMCs.

To gain further insights into the attenuated exocytotic response of Ndrg1$^{-/-}$ BMMCs after coculture with fibroblasts, we next examined several parameters of mast cell activation following Fcε RI signaling. When the expression of mast cell surface markers in Ndrg1$^{+/+}$ and Ndrg1$^{-/-}$ BMMCs before coculture was monitored by flow cytometric analysis, markers of BMMCs, including c-kit (Fig. 8A, a and b) and IgE-bound Fcε RI (Fig. 8A, e and f) were equally expressed in cells of both genotypes. After coculture with fibroblasts, Ndrg1$^{+/+}$ and Ndrg1$^{-/-}$ BMMCs still expressed similar levels of c-kit (Fig. 8A, c and d). Remarkably, the expression of Fcε RI was elevated in cocultured Ndrg1$^{-/-}$ BMMCs (Fig. 8Ag), whereas this increase was negligible in replicate Ndrg1$^{+/+}$ BMMCs (Fig. 8Ah). Accordingly, Ndrg1$^{-/-}$ BMMCs expressed a lower level of Fcε RI than did Ndrg1$^{+/+}$ BMMCs after coculture (Fig. 8A, f and h). Tyrosine phosphorylation of the γ isoforms of PLC, which hydrolyze phosphatidylinositol bisphosphate to

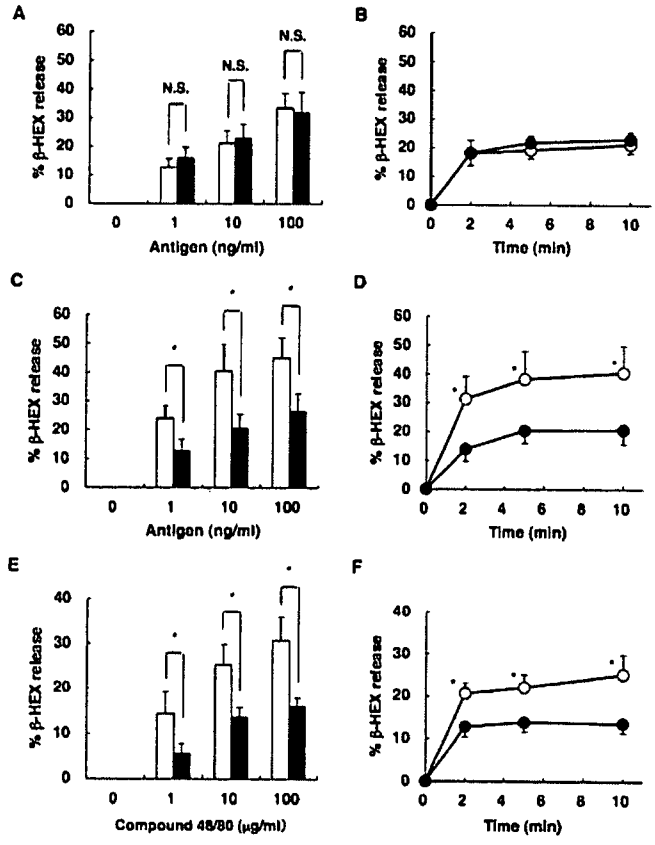

FIGURE 7. The exocytotic response of wild-type and Ndrg1-deficient BMMCs before and after coculture with fibroblasts as assessed by release of •-HEX. Ndrg1• /• (• /• , open symbols) and Ndrg1• /• (• /• , filled symbols) BMMCs before (A and B) and after (C and D) coculture with fibroblasts were preloaded with anti-DNP IgE and stimulated with the indicated concentrations of DNP-BSA (A and C) and with 10 ng/ml DNP-BSA for the indicated periods (B and D). Alternatively, Ndrg1• /• and Ndrg1• /• BMMCs after coculture with fibroblasts were stimulated with the indicated concentrations of compound 48/80 (E) and 10 • g/ml compound 48/80 for the indicated periods (F). Data shown are the mean • SEM of at least six independent experiments with triplicate samples at each point. •, p • 0.05; and ••, p • 0.01 vs Ndrg1• /• BMMCs.

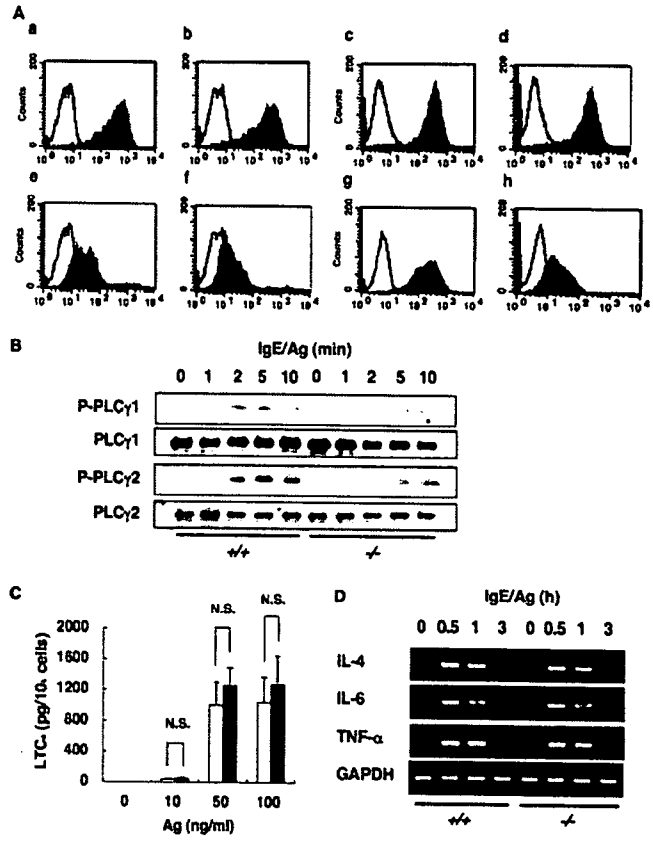

FIGURE 8. Fc•RI signaling of wild-type and Ndrg1-deficient BMMCs after coculture with fibroblasts. A, Surface expression of c-kit and Fc•RI in BMMCs before and after coculture with fibroblasts. Ndrg1• /• (a, c, e, and g) and Ndrg1• /• (b, d, f, and h) BMMCs before (a, b, e, and f) and after (c, d, g, and h) coculture with fibroblasts were incubated with or without 10 • g/ml mouse IgE, and then stained with PE-labeled anti-mouse IgE Ab (e–h). c-kit expression was detected with FITC-labeled anti-mouse c-Kit Ab (a–d). Representative histograms of BMMCs from three independent experiments are shown. B, Tyrosine phosphorylation of PLC•1 or PLC•2 in BMMCs after coculture with fibroblasts. IgE-sensitized BMMCs from Ndrg1• /• (• /•) and Ndrg1• /• (• /•) mice were stimulated with DNP-BSA for indicated times. Lysates from these cells were subjected SDS-PAGE, transferred to nitrocellulose membrane filters, and then immunoblotted with Abs against tyrosine-phosphorylated forms of PLC•1 and PLC•2 (P-PLC•1 and P-PLC•2, respectively). After stripping, the filters were reprobed with anti-PLC•1 or anti-PLC•2 Ab to determine their protein levels. C, LTC_4 production by Ndrg1• /• (open bars) and Ndrg1• /• (filled bars) BMMCs after coculture with fibroblasts. The IgE-sensitized cells were stimulated with the indicated doses of Ab for 30 min. LTC_4 levels in the supernatants were measured by ELISA. N.S., not significant. D, Expression of cytokine mRNAs in BMMCs after coculture with fibroblasts. Total RNAs were extracted from cocultured Ndrg1• /• and Ndrg1• /• following stimulation for the indicated periods with IgE and Ag and then subjected to RT-PCR for IL-4 (30 cycles), IL-6 (25 cycles), and TNF-• (25 cycles) as well as GAPDH (control; 23 cycles) using the respective specific primers.

produce the second messengers inositol triphosphate and diacylglycerol, is an early post-Fc•RI event that is subsequently linked to intracellular $Ca^{2•}$ mobilization and protein kinase C activation (44–46). As shown in Fig. 8B, the phosphorylation of PLC•1 and PLC•2, which occurred within a few minutes after Ag challenge as revealed by immunoblotting with Abs specific for phosphorylated PLC• isoforms, was partially reduced in cocultured Ndrg1• /• BMMCs compared with replicate wild-type BMMCs, although the total amount of each PLC• isoform was indistinguishable between the both genotypes. These results raised the possibility that the reduced Fc•RI-mediated exocytotic response in cocultured Ndrg1• /• BMMCs (Fig. 7) might be at least partly attributable to a defective maturation-associated elevation of Fc•RI expression (Fig. 8A) and, thereby, reduced activation of PLC• (Fig. 8B).

However, the production of cysteinyl LTC_4, an arachidonate-metabolizing product, which depends entirely on an increased intracellular $Ca^{2•}$ level and MAPK (47, 48), was unaffected in Ndrg1• /• BMMCs after coculture (Fig. 8C). In addition, Fc•RI-induced expression of several cytokines including IL-4, IL-6 and TNF-•, an event that depends on the activation of multiple signaling pathways such as protein kinase C, MAPK, NF-•B, NF-AT, or PI3K (49–54), occurred normally in Ndrg1• /• BMMCs even after coculture (Fig. 8D). Consistently, the increase in intracellular $Ca^{2•}$, an upstream event for LT and cytokine generation after Fc•RI cross-linking, was comparable between cocultured Ndrg1• /• and Ndrg1• /• BMMCs (data not shown). These results argue that the residual activation of PLC• is still sufficient for downstream signaling pathways, leading to full eicosanoid synthesis and cytokine expression in cocultured Ndrg1• /• BMMCs. It appears, therefore, that the reduced degranulation in Ndrg1• /• BMMCs may have resulted from a regulatory step(s) other than the receptor-proximal events.

Discussion

Recent reports that overexpression or knockdown of NDRG1 in cultured neoplastic cells alters their proliferation, differentiation, metastasis, and apoptosis statuses (25, 28, 29, 55–58) and that genetic mutations in the Ndrg1 gene cause Schwann cell dysfunction leading to peripheral neuropathy in both human and mouse (30–32) imply that this inducible intracellular protein plays roles in diverse processes linked to these cellular events. Despite its widespread distribution, however, the regulatory expression and functions of NDRG1, particularly in the immune system, have been poorly understood. We previously found that NDRG1 is markedly induced during ex vivo differentiation of IL-3-dependent BMMCs, a relatively immature population of mast cells, into more mature CTMC-like cells that contain safranin-positive secretory granules, produce large amounts of PGD_2, and show sensitivity to G protein-coupled polycationic secretagogues such as compound 48/80 and substance P (14, 15). Although the forcible transfection of NDRG1 into a mast cell-line augmented the exocytotic response (15), an event suggesting the potential ability of this protein to promote the functional maturation of mast cells, the physiological relevance of these observations has still remained elusive. In an effort to gain further insight into the functional roles of NDRG1 in mast cell biology, in the present study we examined mast cell-associated phenotypes of Ndrg1-deficent mice. Our results provided evidence that NDRG1 plays a pivotal role in the terminal maturation and effector function (degranulation) of mast cells in vivo and ex vivo.

Ndrg1$^{-/-}$ mice were partially resistant to passive systemic anaphylaxis, displaying only modest changes in rectal temperature and plasma histamine level in comparison with the replicate Ndrg1$^{+/+}$ littermate control (Fig. 1). Likewise, in the passive cutaneous anaphylactic response Ndrg1$^{-/-}$ mice exhibited attenuated extravasation (an event triggered by mast cell-derived mediators such as histamine and cysteinyl LTs) at the sites of stimuli (Fig. 2), whereas skin mast cells in the null mice showed only minimal degranulation (Fig. 3). The latter observation is supported by the ex vivo experiments showing that PMCs from Ndrg1$^{-/-}$ mice were less sensitive to Fc•RI cross-linking than those from Ndrg1$^{+/+}$ mice (Fig. 4B). In addition to these functional defects, dermal and serosal CTMCs of Ndrg1$^{-/-}$ mice contained fewer and unusual secretory granules (Figs. 3–5), suggesting their immaturity.

Studies using the culture system in which BMMCs differentiate into CTMC-like cells revealed that, although immature BMMCs maintained in IL-3 were virtually identical between the Ndrg1$^{+/+}$ and Ndrg1$^{-/-}$ genotypes, after maturation into CTMC-like cells by coculture with fibroblasts in the presence of SCF the BMMCs showed several notable differences in terms of ultrastructure and function. Thus, as compared with the Ndrg1$^{+/+}$ control, Ndrg1$^{-/-}$ BMMCs after coculture contained aberrant secretory granules that were small and irregular with a paucity of electron-lucent and dense contents (Fig. 6), in agreement with the altered morphology of dermal and serosal CTMCs in Ndrg1$^{-/-}$ mice as mentioned above (Figs. 3–5). In addition, the retarded proliferation of Ndrg1$^{-/-}$ BMMCs in coculture may be a reflection of reduced mast cell number in vivo. The coculture was accompanied by augmented Fc•RI-mediated exocytosis in Ndrg1$^{-/-}$ BMMCs, whereas this event did not occur appreciably in replicate Ndrg1$^{+/+}$ BMMCs (Fig. 7). The surface expression levels of c-kit, CD34, and Sca-1 on BMMCs were similar between the two genotypes irrespective of coculture, indicating that NDRG1 does not affect the expression of these early mast cell surface markers (data not shown). Interestingly, the expression of Fc•RI was elevated in Ndrg1$^{-/-}$ but not in Ndrg1$^{+/+}$ BMMCs after coculture (Fig. 8A), and this change appears to be associated with reduced PLC• phosphorylation, an Fc•RI-proximal event, in Ndrg1$^{-/-}$ BMMCs (Fig. 8B). However, almost normal LT synthesis and cytokine expression in cocultured Ndrg1$^{-/-}$ BMMCs (Fig. 8, C and D) argues against the contribution of the moderate changes in these receptor-proximal events to the reduced exocytosis. It is also notable that the exocytotic response to compound 48/80, a G_i-coupled secretagogue to which response became apparent after coculture, as well as the response to ionomycin, a Ca^{2+} ionophore, was also partially reduced in cocultured Ndrg1$^{-/-}$ BMMCs compared with replicate Ndrg1$^{+/+}$ cells (Fig. 7, E and F). These results are in agreement with our previous observation that the overexpression of NDRG1 in RBL-2H3 mastocytoma led to a marked enhancement of degranulation but not eicosanoid synthesis following various stimuli (15). Thus, it is speculated that NDRG1 plays a role in the divergent signaling at the point of convergence or beyond leading to exocytosis.

Whereas it has been reported that NDRG1 shows cytoplasmic, nuclear, and even mitochondrial localization and often shuttles between the cytoplasm and the nucleus according to cell type, stimulus, and cell cycle stage (15, 25, 39, 59, 60), in the present study we found that in mast cells NDRG1 exhibits a unique punctate distribution in the cytoplasm, particularly around secretory granules (Fig. 4). A likely explanation for this location is that NDRG1 binds to certain proteins or lipid components that are enriched in the mast cell granule membranes. Interestingly, by means of yeast two-hybrid screening we and others have recently found that NDRG1 has the potential capacity to associate with several cellular proteins, such as HSC70, PICK-1, p47, Pra1, RTN-1C, and Aip-1, all of which are known to participate in cellular events related to membrane transport and fusion (59, 60). The interrelated protein trafficking of NDRG1 binding partners points to its possible involvement in the complex network of vesicular transport. In relation to this, the blood level of high-density lipoprotein is reduced in CMT4D patients harboring the R148X mutation in the Ndrg1 gene (60), and several genetic disorders of lipid vesicular transport cause the CMT-like peripheral neuropathy that accompanies demyelination (61, 62). These facts raise the possibility that the neuropathic phenotype of Ndrg1 mutation might be due to a perturbation of lipid trafficking and membrane transport in Schwann cells. Moreover, high steady-state expression of NDRG1 is found in renal proximal tubular and intestinal epithelial cells, which actively transport vesicles with polarity from apical to basolateral membranes (39). Thus, apart from the regulatory role of NDRG1 in the terminal maturation of mast cells, the reduced exocytosis of Ndrg1-null mast cells may be indicative of an additional role of this protein in the regulation of the secretory process. Supporting this idea, our recent GeneChip analysis of Ndrg1$^{-/-}$ vs Ndrg1$^{+/+}$ BMMCs after coculture has revealed that Ndrg1 deficiency leads to a marked reduction in the expression of a panel of genes related to cytoskeletal organization and rearrangement (data not shown) that could have a deep impact on cellular shape, cell division, membrane integrity and fusion, vesicular transport, and even exocytotic function. A possible functional link of NDRG1 with each component of those GeneChip-identified genes is now under investigation at molecular levels.

The finding that there are fewer electron-dense secretory granules in CTMCs in Ndrg1$^{-/-}$ mice than in Ndrg1$^{+/+}$ mice is suggestive of substantial changes in the granule contents. Because • 50% of the weight of a PMC consists of protease/proteoglycan complexes that are packaged in the cell granules, we evaluated for